

SCALED-UP PURIFICATION OF POLY(ACRYLIC ACID)-BLOCK-
POLYSTYRENE NANOPARTICLES USING TANGENTIAL FLOW FILTRATION:
A FEASIBILITY STUDY

A Thesis

by

MAHSA MINAEIAN

Submitted to the Office of Graduate and Professional Studies of
Texas A&M University
in partial fulfillment of the requirements for the degree of

MASTER OF SCIENCE

Chair of Committee,	Karen L. Wooley
Committee Members,	James D. Batteas
	Jodie L. Lutkenhaus
Head of Department,	Simon W. North

December 2019

Major Subject: Chemistry

Copyright 2019 Mahsa Minaeian

ABSTRACT

Use of polymeric nanoparticles has gained significant interest in recent years for a wide spectrum of applications such as drug delivery, cell imaging, environmental remediation, and, electronics. However, many of these nanoparticles have been mainly synthesized at the laboratory scale. Large scale synthesis of these nanoparticles in a cost-effective and reliable fashion could significantly expand their industrial use. In many cases, self-assembly of block polymers into different morphologies involves a transition from a solvated polymer in an organic solvent to a fully aqueous system. Here, the feasibility of using tangential flow filtration (TFF) to scale-up the solution-state transition was studied.

A custom-designed and chemically resistant experimental TFF system was built. Nine TFF experiments were performed to study the effects of change of transmembrane pressure, nanoparticles concentration, and hydrophobic/hydrophilic block ratio on solvent removal and nanoparticle size evolution during the diafiltration process. In addition, three batch dialysis experiments were performed to understand the possible extent of scale-up using the proposed system. The designed experimental setup had considerable chemical resistance to many solvents and could be used to conduct small-molecule removal, scale-up, and concentration processes on a wide range of polymers.

Feasibility of use of TFF for purification of amphiphilic polymeric nanoparticles with core-shell morphology was demonstrated. Solvent exchange using TFF was considerably faster compared to the traditional batch dialysis system. In TFF experiments,

the organic solvent concentration reached the minimum level after 1 hour of in-flow filtration, while it took around 6 hours to reach similar levels of solvent exchange in the batch setting. In addition to an order of magnitude higher processing volumes of TFF compared to dialysis, further scale-up of the TFF process is easily achievable with increasing the membrane area. As expected, higher transmembrane pressure resulted in faster organic solvent removal. The initial nanoparticles concentration had a significant effect on the diameter of the formed structures during the TFF purification, which affected the required purification time. A high ratio of hydrophobic to hydrophilic blocks in a block copolymer increases the chance of precipitation of nanoparticle during TFF, which might terminate the process.

DEDICATION

To my parents, Hoori and Mohsen, and my husband, Peyman

ACKNOWLEDGEMENTS

I am grateful for my advisor, Dr. Karen L. Wooley, for her advice and generous support throughout the course of this research. I would also like to thank my committee members, Dr. Batteas and Dr. Lutkenhaus, for their valuable time, guidance and support.

Thanks also go to Wooley group members for making my time at Texas A&M University a memorable one. In particular, Dr. Rachel Letteri, Dr. Fuwu Zhang, Mei Dong and Yue Song for their guidance and support during my research. I want to express my appreciation to my friends, Sopida Thavornpradit, David Tran, and Benjamin Demor for their support and all of the enjoyable moments and experiences we had together.

I am thankful to Dr. Yohannes Rezenom for his assistance with performing gas chromatography experiments and valuable scientific discussions. Also, William Merka and William Seward, research instrumentation specialists from the chemistry department glass shop and machine shop, who helped with the fabrication of different pieces for the diafiltration system.

My heartfelt thanks go to my family, especially my parents for their love, support and care. Last but not least, I would like to thank my husband, Peyman Heidari, for his encouragement, patience, and unconditional love.

CONTRIBUTORS AND FUNDING SOURCES

Contributors

This work was supervised by a thesis committee consisting of Professor Karen L. Wooley (advisor) and Professor James D. Batteas of the Department of Chemistry and Professor Jodie L. Lutkenhaus of the Department of Chemical Engineering.

All of the work conducted for the thesis was completed by the student independently.

Funding Sources

This work was made possible in part by the National Science Foundation under Grant Number “DMREF-1629094 and DMR-1507429”, and Robert A. Welch Foundation through the W. T. Doherty-Welch Chair in Chemistry, Grant Number A-0001. Its contents are solely the responsibility of the authors and do not necessarily represent the official views of the National Science Foundation or the Robert A. Welch Foundation.

TABLE OF CONTENTS

	Page
ABSTRACT	ii
DEDICATION	iv
ACKNOWLEDGEMENTS	v
CONTRIBUTORS AND FUNDING SOURCES.....	vi
TABLE OF CONTENTS	vii
LIST OF FIGURES.....	ix
LIST OF TABLES	xi
CHAPTER I INTRODUCTION AND LITERATURE REVIEW	1
Importance and Motivation.....	1
Hybrid Organic/Inorganic Nanostructures for Water Remediation	2
Purification.....	5
Tangential Flow Filtration.....	8
Scope of Work.....	10
CHAPTER II SYNTHESIS AND METHODOLOGY.....	11
Materials.....	11
Characterization techniques	12
Synthesis of Amphiphilic Block Copolymer and Self-Assembly.....	14
Synthesis of PAA ₂₂ -b-PS ₁₄₁	15
Diafiltration System (DFS) Experimental Setup.....	19
Initial Setup and Pump Calibration	21
Cleaning of the Membrane Cassette.....	23
Measurement of Water Permeability.....	23
Preparation of DFS for Diafiltration Experiment.....	24
Transmembrane Pressure Optimization	25
THF Measurements using HSGC.....	26
Hydrodynamic Size Measurement using DLS	28
Experimental Design.....	28

CHAPTER III RESULTS AND DISCUSSION	31
In-flow Purification of Block Copolymers Assemblies using TFF.....	31
Tangential Flow Filtration vs. Batch Dialysis.....	34
Effects of Transmembrane Pressure on TFF.....	36
Effects of Initial Concentration of Nanoparticles on TFF.....	39
Effect of Block Ratio on TFF.....	42
Effect of Block Ratio on TFF at Concentration of 2.5 mg/mL	42
Effect of Block Ratio on TFF at Concentration of 1.0 mg/mL	45
CHAPTER IV CONCLUSIONS AND FUTURE WORK.....	48
REFERENCES.....	51
APPENDIX A HYDRODYNAMIC SIZE MEASUREMENTS (DLS).....	55
APPENDIX B NOMENCLATURE	62

LIST OF FIGURES

	Page
Figure II.1 (A) SEC traces of PtBA ₂₂ in blue and PtBA ₂₂ - <i>b</i> -PS ₁₄₁ in black (B) IR spectra of PtBA- <i>b</i> -PS in black and PAA- <i>b</i> -PS in red.....	17
Figure II.2 (A) Schematic of the experimental setup. (B) Picture of the diafiltration system which consists of (a) syringe pump for buffer addition, (b) feed tank, (c) peristaltic pump, (d) feed pressure gauge, (e) permeate flow rate measurement scale, (f) cassette holder and cassette, (g) retentate pressure gauge, (h) needle valve for pressure regulation, and (i) sampling port.	20
Figure II.3 Pump calibration measurements with error bar at each data point shown in red.	22
Figure II.4 (A) An example of TMP excursion plot (B) TMP excursion plot for diafiltration experiment of PAA ₄₇ - <i>b</i> -PS ₂₃₅ nanoparticles	26
Figure II.5 HSGC calibration curve	27
Figure III.1 Solvent exchange in 50% THF solution without nanoparticles is much faster solutions with nanoparticles (PAA ₆₄ - <i>b</i> -PS ₆₀ and PAA ₄₇ - <i>b</i> -PS ₂₃₅). (A) Absolute and (B) logarithmic relative concentration (sample THF concentration/initial THF concentration).	33
Figure III.2 Comparison of tangential flow filtration and traditional batch dialysis for purification of nanoparticles solution in 50:50 THF:water solution based on (A,C,E) logarithm of relative residual THF concentration and (B,D,F) changes of number-averaged diameter of nanoparticles over time.	35
Figure III.3 Increasing TMP from 16 psig to 26 psig decrease the required time for diafiltration of PAA ₄₇ - <i>b</i> -PS ₂₃₅ assemblies in 50% THF in water solution based on (A) absolute and (B) logarithmic relative concentration data.	38
Figure III.4 Change of TMP has negligible effect on number-averaged diameter of PAA ₄₇ - <i>b</i> -PS ₂₃₅ nanoparticles.	39
Figure III.5 Rate of organic solvent removal during diafiltration process of PAA ₆₄ - <i>b</i> -PS ₆₀ assemblies was similar for solution with concentration of 2.5 mg/mL and 4.0 mg/mL, and was slower for 1.0 mg/mL. (A) Absolute and (B) logarithmic relative concentration data.	40
Figure III.6 The hydrodynamic size evolution for PAA ₆₄ - <i>b</i> -PS ₆₀ assemblies with 1.0, 2.5 and 4.0 mg/mL initial polymer concentrations. Diameter of micelles	

formed in solution of 4.0 mg/mL concentration were almost double the ones with lower concentrations.....	41
Figure III.7 Formation of precipitates at the feed inlet of the membrane holder.....	44
Figure III.8 Comparison of residual organic solvent content in the retentate samples collected from diafiltration process of different polymeric nanoparticles (PAA ₆₄ - <i>b</i> -PS ₆₀ , PAA ₂₂ - <i>b</i> -PS ₁₄₁ and PAA ₄₇ - <i>b</i> -PS ₂₃₅ with different block ratio at concentration of 2.5 mg/mL. (A) Absolute and (B) logarithmic relative concentration data.....	44
Figure III.9 The hydrodynamic size evolution of PAA ₆₄ - <i>b</i> -PS ₆₀ , PAA ₄₇ - <i>b</i> -PS ₂₃₅ , and PAA ₂₂ - <i>b</i> -PS ₁₄₁ nanoparticles during TFF (conc.= 2.5 mg/mL).....	45
Figure III.10 Comparison of residual organic solvent in the retentate samples during purification of PAA ₆₄ - <i>b</i> -PS ₆₀ , PAA ₈₅ - <i>b</i> -PS ₁₈₂ and PAA ₄₇ - <i>b</i> -PS ₂₃₅ at concentration of 1.0 mg/mL. (A) Absolute and (B) logarithmic relative concentration data.....	46
Figure III.11 The hydrodynamic size evolution of PAA ₆₄ - <i>b</i> -PS ₆₀ , PAA ₄₇ - <i>b</i> -PS ₂₃₅ , and PAA ₈₅ - <i>b</i> -PS ₁₈₂ nanoparticles during TFF (conc.= 1.0 mg/mL).....	47

LIST OF TABLES

	Page
Table II.1 Performed experiments to study the effect of transmembrane pressure (A), PS/PAA block ratio (C1, C2.5), and nanoparticles concentration (D) on the TFF process. In addition, (B) experiments were compared to batch dialysis experiments.....	30

CHAPTER I

INTRODUCTION AND LITERATURE REVIEW

Importance and Motivation

The scaled-up production of nanotechnological materials is of importance fundamentally, in defining parameters and processes by which to achieve rapid fabrication with reproducibility, and practically, in terms of their broad applicability. The solution-state supramolecular assembly of amphiphilic block polymers often involves a transition of organic polymers from a solvated state in an organic solvent to a dispersed phase in water, which triggers their multi-molecular aggregation to afford well-defined nanoscopic structures by a relatively simple process. The resulting materials may exist with a variety of morphologies, for which an amphiphilic core-shell morphology is similar to many structures found in nature and has characteristics that provide for performance in a range of applications, from drug delivery to water remediation. A well-known class of nanomaterials with a core-shell morphology are shell cross-linked knedel-like nanoparticles (SCKs),^{1, 2} which are polymeric micelles cross-linked through the shell region of the particles. SCKs have received considerable interest due to their well-defined structures and tunable physical and chemical functionalities.^{3, 4} The general synthetic approach for the preparation of SCK polymer assemblies involves the synthesis of amphiphilic block copolymers followed by their self-assembly into micelles and covalent cross-linking, which reinforces the stability of the nanostructure.⁵ However, bulk processes for the preparation of such materials are impractical on large scales. This thesis

focuses upon flow systems for the scaled-up solution-state transition that would allow for production and purification of nanoscopic polymer assemblies.

Hybrid Organic/Inorganic Nanostructures for Water Remediation

The marine environment has been burdened with pollution from oil spills for decades^{6, 7, 8}. Petroleum extraction, processing, and transport increase the risk of pollution from discharge into seawater. Although traditional collectors, such as booms and skimmers are successful for the removal of large amounts of oil, they are not effective for thin oil layers on the water surface or sub-surface pools of oil. Oil recovery has been enhanced by the emergence of nanotechnology for water remediation. Nanotechnology facilitates the design of materials with specific properties through tailoring the structures and compositions, including the construction of macromolecules of increasing size and complexity at the nanoscale.

Magnetic shell cross-linked knedel-like nanoparticles (MSCKs) designed by Pavía-Sanders *et al.*⁹ have shown desirable efficiency in oil cleanup from aqueous environments with an uptake ratio of 10 mg of oil per 1 mg of MSCK. These well-defined hybrid networks were made from a poly(acrylic acid)-*b*-polystyrene (PAA-*b*-PS) organic domain and a magnetic iron oxide nanoparticle inorganic domain, which promoted oil capture and provided convenient recovery of loaded materials. Magnetomicelles with a number-averaged hydrodynamic diameter of 70 nm were fabricated through co-assembly of amphiphilic block copolymers of PAA₂₀-*b*-PS₂₈₀ and oleic acid-stabilized iron oxide nanoparticles. Due to the higher uniformity of the resulting nanoparticles in the

magnetomicelle morphology, it was chosen over other architectures such as magnetopolymersomes and magneto-core shell assemblies.¹⁰ The core-shell architecture of MSCK is composed of a hydrophilic surface which aids dispersing in water and a hydrophobic core for entrapment of hydrocarbons.

Synthesis of MSCKs started with the synthesis of its organic domain. The diblock copolymer of *PtBA-b-PS* was synthesized by sequential ATRP of *tert*-butyl acrylate and styrene in anisole and in the presence of CuBr and PMDETA (*N,N,N',N',N''*-pentamethyldiethylenetriamine) at 55 °C and 95 °C, respectively.¹¹ Deprotection of the carboxylic acid by removal of the *tert*-butyl group using trifluoroacetic acid produced the amphiphilic block copolymer of *PAA-b-PS*.

The inorganic component of MSCKs, iron oxide nanoparticles, was synthesized using a thermal decomposition method.¹² Iron (III) acetylacetonate and 1,2-hexadecanediol were reacted in the presence of oleic acid and oleyl amine as surfactant and benzyl ether as the reaction solvent. The reaction was conducted in three 1-hour periods at temperatures of 140 °C, 200 °C, and 250 °C, sequentially. After precipitation in ethanol, the resulting nanoparticles were characterized by transmission electron microscopy (TEM) and superconducting quantum interface device (SQUID).

Following synthesis of MSCKs, a similar polymeric nanoparticle was designed by Flores *et al.* through the coupling of amine-functionalized iron oxide nanoparticles and pre-prepared SCK micelles to form magnetically active hybrid networks (MHNs). Cargo space to capture hydrocarbons were formed within the interconnected SCKs. However, MHNs demonstrated lower oil uptake capacities compared to MSCKs.¹³

Co-assembly into micelles was performed by a modified process of a previously established method proposed by Kim *et al.*¹⁴ In this modified method, initially the block copolymers and iron oxide nanoparticles were dissolved in a 1:1 ratio of *N,N*-dimethylformamide (DMF) and tetrahydrofuran (THF). Then, this mixture and the same volume of water were simultaneously added to a vessel containing nanopure water (0.33 × volume) concurrently and dropwise. Since water is a selective solvent for PAA blocks and anti-solvent for iron oxide nanoparticles and PS blocks, the addition to water led to magnetic micelle assembly with hydrophobic core protected by hydrophilic PAA block shells. After micelle formation, the solution was transferred to a fully aqueous system through dialysis against nanopure water for 24 hours. According to TEM analysis, an average number of 75 magnetic particles were incorporated within the core of each micelle. The average number of nanoparticles can be adjusted by changing the initial concentration of nanoparticles relative to the concentration of copolymers.¹⁵

Cross-linking through PAA chains via amidation of acrylic acid groups was the final step of MSCKs fabrication. Nominally 25% of the acrylic acid repeat units were cross-linked using (2,2'-ethylenedioxy)-bis(ethylamine) and 1-(3-(dimethylamino)propyl)-3-ethylcarbodiimide methiodide (EDCI). Unreacted cross-linking agent and reaction byproducts were removed by extensive dialysis against nanopure water. TEM, atomic force microscopy (AFM), dynamic light scattering (DLS), and infrared spectroscopy (IR) were used for characterization of MSCKs. Purification and removal of the non-selective solvent are among the time-consuming steps of MSCKs fabrication during both co-assembly and cross-linking processes.

Purification

Purification is usually needed to remove residual reactants, by-products, and impurities from the solution after obtaining nanoscale polymer assemblies. Some of these undesirable materials are organic solvents, polymerization initiators, oil, salts, excess stabilizing agents, surfactants, and large polymer aggregates. Several methods have been previously proposed for purification of nanoparticles suspensions at the laboratory scale. Some of these methods are dialysis,¹⁶ evaporation under reduced pressure,¹⁷ ultracentrifugation,¹⁸ filtration through mesh,¹⁹ ultrafiltration,²⁰ and gel filtration.²¹

During evaporation under reduced pressure, volatile organic solvents are removed from the solutions by decreasing the pressure of the system. The pressure is decreased to lower the boiling point of the solvents and therefore reducing the need for high temperatures. Low temperatures are generally preferred due to the possibility of degradation of many polymers at high temperatures.^{22, 23} Filtrations through mesh is usually used to remove large polymer aggregates from nanoparticles suspensions that have formed during preparations.²⁴ While centrifugation can be used to remove large particles from the suspensions, it is not recommended to be used with small assemblies. Ultracentrifugation is similar to centrifugation but at very high speed. This method exploits the dependence of particle sedimentation rate on even small changes in particle size and shape, which is linked to viscous hydrodynamics.²⁵ After ultracentrifugation, the dispersing fluid containing all the impurities can be removed and the remaining solution can be re-dispersed in new pure fluid. Generally, this step is applied several times to reach the desired levels of purification. However, nanoparticles are not always easy to re-

disperse.^{26, 27} These methods are generally time-consuming or sensitive to operational conditions, which inhibits their use for industrial-scale purification.²⁸

In purification by dialysis, membranes usually made from cellulose with a variable molecular weight cut off are used to enable diffusion of molecules below the cut off level between solutions separated by the membrane, which is driven by the concentration gradient. Efficient dialysis requires a long purification period and a large volume of buffer. Therefore, use of dialysis in large-scale purification processes is hindered from an economical point of view. Alternative methods based on cross-flow filtration, diafiltration, ultrafiltration, and microfiltration were suggested.^{29, 30, 31, 27}

Dialysis and filtration separate components based on their size using permeable membranes. However, the driving forces behind these methods are different. In dialysis, the concentration gradient between inside and outside of the membrane results in the removal of solvent and other small molecules from the solution. The production of macromolecules with well-defined morphologies at the industrial scale requires a large-scale purification process. However, because of the batch nature of dialysis, it is a slow process. Dialysis is often appropriate for organic solvent removal at the small-scale laboratory synthesis.

The pressure difference across the membrane is the driving force of separation during the filtration process. Filtration is classified into tangential and normal flow filtration. Tangential flow filtration (TFF), also referred as cross-flow filtration, is a filtration technique where feed solution flows tangentially along the surface of the membrane. Generally, during the filtration process solvent is added directly to the feed

tank for desalting or solvent exchange. Ultrafiltration membranes that are usually used for diafiltration processes are classified based on their nominal molecular weight cutoff (MWCO) ranging between 1 kDa-1000 kDa. The MWCO is the largest size of particles that can pass through the pores of the membrane during the separation process.³² Filtration is usually a significantly faster method compared to dialysis due to the applied pressure difference and the cross-membrane flow. The continuous nature of diafiltration makes it a desirable candidate for economical scale-up of the purification process.

During the filtration process, the transmembrane pressure drives a portion of the feed (e.g. a nanoparticle suspension) that is smaller than the membrane pores to travel through the membrane. This separates the feed solution into retentate and permeate.^{33, 34} A major problem of the traditional normal flow filtration (NFF) or dead-end filtration is membrane fouling, which limits the use of this method at the large scale. Membrane fouling is due to the formation of filter cake over the membrane. Formation of a nanoparticle cake when a suspension is pressed through a membrane. The cake can be irreversible if the adhesion of the particles on the membrane is stronger than its repulsion, which can dramatically decrease membrane permeability.³⁵ The cake formation issue can be alleviated through utilizing filtration with suction,³¹ using hydrophilic membranes,³⁶ or by using tangential flow filtration.

Membrane fouling in TFF is noticeably less compared to NFF. This is due to the direction of the fluid flow, which is parallel to the surface of the membrane in TFF. The normal flow towards the surface of the membrane in NFF causes plugging due to the accumulation of particles on the membrane surface. Therefore, TFF suffers less from

membrane fouling and therefore increases the efficiency of the filtration process. TFF has been extensively used in biotechnology. Specifically, purification and recovery of biomolecules, such as protein³⁷, DNA³⁸, and viruses³⁹ have been reported.

Tangential Flow Filtration

Recently, application of TFF for nanoparticles processing has gained more interest due to the continuous nature of this process and easier operational procedure.^{40, 34, 41-44, 45} For example, in a comparative study of use of TFF and the commonly used ultracentrifugation technique for removal of excess polyvinyl alcohol (PVA) from nanoparticles dispersions, it was shown that a TFF capsule can efficiently remove more than 90% of PVA molecules in 2.8 hours.⁴² The TFF purification process found to be more efficient than dialysis and ultracentrifugation with less impact on the yield, size, and stability of nanoparticles. In addition, neither membrane fouling, nor particle caking was observed during the TFF process. It was shown that TFF has the potential for purification scale-up due to the possible increased efficiency at higher transmembrane pressures and the possibility of significantly increasing the membrane surface area to expedite the process at the industrial scale.⁴² In a similar study, lipid-based nanoparticles produced through a single-step flash nanocomplexation process were successfully purified and concentrated using the TFF procedure in a scalable manner.⁴¹

Use of the TFF system was shown to be a highly efficient method for the removal of macromolecules from ferrofluid suspensions without changing the surface properties or the hydrodynamic sizes of the particles. In addition, it was shown that TFF can

concentrate the solutions up to four times without compromising colloidal stability in biorelevant media, which can greatly enhance the magnetic properties of the suspensions.⁴⁶ In addition, the crossflow purification of poly(D,L-lactic acid) (PLA) nanoparticles prepared by an emulsification–diffusion technique using polyvinyl alcohol (PVAL) or poloxamer 188 (P-188) has been investigated. It was shown that nanoparticles prepared with PVAL can be filtered without fusion.⁴⁷ In another study, TFF was utilized for removal of impurities from suspensions of polyethylene oxide stabilized nanoparticles to values below FDA required limits. It was shown that smaller nanoparticles resulted in higher filter cake resistance, which agrees with the expected change of permeability with particle diameter. In addition, experiments with rigid poly(methyl methacrylate) sphere showed no growth of a filter cake until a critical value of transmembrane pressure (TMP=7.5 psia) was applied. Above the critical TMP level, the filter cake resistance grew linearly.⁴⁰

Tangential flow filtration has been investigated as a suitable technique for nanoparticles solution purification with possible adaptation for scaled-up applications.^{48,49,28} For example, Sun *et al.*⁴⁸ developed a process consisting of alkaline lysis, tangential flow filtration (TFF), purification by anion exchange chromatography, hydrophobic interaction chromatography and size exclusion chromatography for large-scale purification of pharmaceutical-grade plasmid DNA. The process was scaled up to yield 800 mg of pharmaceutical-grade plasmid DNA and reached an overall yield of 48%.⁴⁸ In another study, the possibility of scale-up of an ultrafiltration system for recovery of entomotoxicity components from *Bacillus thuringiensis* fermented wastewater sludge

broth was explored. The optimal operational parameters for the process were reported and it was stated that the dynamic resistance of the cake layer was as a key parameter that should be considered to estimate the required power for scale-up of any feed. In conclusion, scale-up of the TFF system used by the starch industry wastewater was claimed to be easily achievable.³⁴ A holofiber-based TFF system was used to scale up the production of human mesenchymal stem/stromal cells of extracellular vesicle (MSC-EVs), which have been recently used in hundreds of clinical trials. The authors claimed that the system was scalable up to several 1000 liters, which is significantly higher than the traditional methods of purification.⁵⁰ In-flow filtration has shown great potential for scaled-up purification of solutions of nanoparticles compared to more traditional, laboratory-scale methods such as dialysis.

Scope of Work

The use of the tangential flow filtration process for organic solvent removal was studied. The main goal of this thesis is to examine the feasibility of scale-up of the purification step during the production of polymeric nanoparticles of PAA-*b*-PS using TFF. In addition, evolution of diameter of nanoparticles throughout the completion of the assembly process and transition to fully aqueous system was analyzed. The effect of change of transmembrane pressure, nanoparticles concentration, and hydrophobic/hydrophilic block ratio on the efficiency of the solvent exchange process using TFF were explored.

CHAPTER II

SYNTHESIS AND METHODOLOGY

A custom-built tangential flow filtration (TFF) system was designed to study the solvent transition from PAA-*b*-PS nanoparticle in 50:50 (by volume) THF and water solution to fully aqueous system. Retentate fluid was sampled regularly during diafiltration. The samples were characterized by headspace gas chromatography (HSGC) for assessment of THF concentration and by DLS for measurement of the hydrodynamic size of nanoparticles.

Materials

All chemicals were purchased from Aldrich Chemical Co. and used without further purification unless otherwise noted. Styrene and *tert*-butyl acrylate monomers were purified through a basic alumina plug to remove the stabilizer. Nanopure water (18.2 M Ω -cm) was obtained from an EMD Millipore Milli-Q water filtration system. Tetrahydrofuran (HPLC grade) (THF) was purchased from Thermo Fisher Scientific and used as received.

Dialysis membrane tubing with a molecular weight cut-off (MWCO) of 6-8 kDa was purchased from Spectrum Laboratories, Inc. and presoaked in nanopure water before use at room temperature. Pellicon 3 cassette with Ultracel membrane with nominal molecular weight cutoff of 10 kDa and filtration area of 88 cm² (P3C010C00) was purchased from EMD Millipore. The Masterflex precision variable-speed pump drive (07528-10) with a PTFE pump head (EW-77390-00) and PTFE pump tubing, 4mm ID,

6mm OD, were purchased from Cole-Parmer, USA. Tygon tubing with FEP-lining on the wetting side with 1/4" ID and 3/8" OD was purchased from Cole-Parmer. A Parker 316 stainless steel inline process needle valve with PTFE stem seal and 1/4" NPT male inlet/outlet port, with a pressure resistance of 5000 psi (pounds per square inch) was used for pressure regulation. A custom 2-liter glass feed reservoir was designed and fabricated in TAMU, Chemistry Glass Shop and Machine Shop. Valves, connectors, and tubing made from solvent resistance materials (polypropylene, nylon, polytetrafluoroethylene (PTFE), polyvinylidene fluoride (PVDF), or Stainless Steel) were purchased from either McMaster-Carr, Cole-Parmer, or US plastic.

Characterization techniques

^1H NMR and ^{13}C NMR spectra were recorded on a Bruker 400 spectrometer interfaced to a LINUX computer using VNMR-J software, and spectra were processed with MestReNova software Mestrelab Research S.L. Samples were prepared as solutions in CDCl_3 or $d_8\text{-THF}$ and solvent protons were used as internal standard. Fourier transform infrared (FTIR) spectra were recorded on an IR-Prestige-21 system (Shimadzu Corp., Japan). Data were analyzed using the IRsolution software. The molar mass and molar mass distribution (or dispersity, D) were determined by size exclusion chromatography (SEC), conducted on a system equipped with Waters model 1515 isocratic pump (Waters Chromatography, Inc.) and a model 2414 differential refractometer with a three-column set of Polymer Laboratories, Inc. Styragel columns ($\text{PL}_{\text{gel}} 5 \mu\text{m}$ Mixed C, 500 \AA , and 104 \AA , $300 \times 7.5 \text{ mm}$ columns) and a guard column ($\text{PL}_{\text{gel}} 5 \mu\text{m}$, $50 \times 7.5 \text{ mm}$). The differential refractometer was calibrated with Polymer Laboratories, Inc., polystyrene standards (300-

467,000 Da). Polymer solutions were prepared at a concentration of *ca.* 3 mg/mL in THF (with 1% v/v toluene as a flow rate marker) and filtered through a 0.45 μm PTFE filter before injection. After system equilibration at 40 °C in THF, which served as eluent, injection volume of 200-300 μL of polymer samples were passed through the SEC system at a flow rate of 1.00 mL/min. Data were analyzed using Empower Pro software from Waters Chromatography, Inc. DLS measurements were conducted using a Zetasizer Nano ZS instrument (Malvern Panalytical Ltd., Malvern, UK) equipped with a laser diode operating at 633 nm. The scattered light was detected at 173° and the photomultiplier aperture and attenuator were adjusted automatically. A Malvern glass square cell (12 mm OD) was used due to its resistance to organic solvent containing samples. The particle size distribution and distribution averages were calculated using particle size distribution analysis routines in Zetasizer 7.13 software. The number of accumulations and measurements duration were adjusted automatically, and all measurements were repeated twice. Here, the number-average is reported as the diameter average of the particle while intensity-average and volume-average are not reported.

THF concentration was quantified by Trace GC Ultra (Thermo Fisher Scientific) with a DB-5MS GC column (30 m \times 0.25 mm ID, 0.25 μm film thickness) coupled to a DSQ II mass spectrometer. The GC-MS (gas chromatography-mass spectrometry) was equipped with TriPlus HS autosampler which enables headspace gas chromatography. The data was acquired using Xcalibur 3.0.63 and analyzed using Qual Browser.

Synthesis of Amphiphilic Block Copolymer and Self-Assembly

Amphiphilic diblock copolymers were synthesized through previously reported conditions.¹¹ In order to synthesize the amphiphilic block copolymer of PAA-*b*-PS, poly(*tert*-butyl acrylate) (PtBA) was synthesized from *tert*-butyl acrylate monomer via atom transfer radical polymerization (ATRP) at 55 °C using ethyl 2-bromoisobutyrate as initiator, copper(I) bromide (CuBr) and *N,N,N',N',N''*-pentamethyldiethylenetriamine (PMDETA) as catalyst system. Subsequently, the resulting polymer went through another ATRP with styrene as the monomer at 90 °C to afford block copolymer of PtBA-*b*-PS. Homo- and diblock polymers were characterized by NMR and gel permeation chromatography (GPC) for the degree of polymerization, molar mass and molar mass distribution (dispersity). Afterward, the *tert*-butyl group was deprotected with the aid of trifluoroacetic acid (TFA) and amphiphilic diblock of PAA-*b*-PS was produced, characterized by FTIR and NMR. To obtain nanoparticles, solution-state self-assembly was performed by dissolving the block copolymer of PAA-*b*-PS in a non-selective solvent, such as THF, which is a good solvent for both PAA and PS blocks. Afterward, a selective solvent for PAA block (water) was slowly added to the resulting solution. Finally, solvent exchange was conducted on the resulting assemblies in 50% THF in water through tangential flow filtration or batch dialysis to obtain stable nanoparticles in fully aqueous systems. In the following section, synthesis of PAA₂₂-*b*-PS₁₄₁ is discussed in detail as an example.

Synthesis of PAA₂₂-b-PS₁₄₁

Synthesis of Poly(*tert*-butyl acrylate)₂₂ (PtBA₂₂) via ATRP

tert-Butyl acrylate (30 eq, 4.99 g, 38.9 mmol), ethyl 2-bromoisobutyrate (1 eq, 253 mg, 1.3 mmol), PMDETA (1.5 eq, 339 mg, 2.0 mmol) and anisole (5 mL) were loaded in a flame dried 50-mL Schlenk-flask equipped with a magnetic stir bar. The reaction flask was sealed with a rubber septum and the solution was degassed by three cycles of freeze-pump-thaw (FPT). CuBr catalyst (1.6 eq, 304 mg, 2.1 mmol) was added to the frozen reaction mixture under nitrogen gas flow and two additional cycles of FPT were performed. The reaction vessel was then allowed to warm up to room temperature and became homogenous through stirring for 10 minutes. Polymerization started by placing the flask into a preheated oil bath (55 °C). Aliquots were collected periodically and analyzed by ¹H NMR spectroscopy to monitor the polymerization. As the expected monomer conversion was reached after 2 h, the polymerization was quenched by immersing the reaction flask into liquid nitrogen and exposure to air. After evaporation of anisole, 20 mL THF was added to the reaction mixture and the catalyst was removed by filtering through a neutral alumina plug. The resulting product was purified by precipitation into cold 90:10 methanol:water mixture (2×). The precipitates were dried overnight under high vacuum on the Schlenk line to afford 4.07 g of PtBA₂₂ as a pale yellow solid, giving 85% yield of the 96% monomer conversion. M_n (NMR) = 3.0 kDa, M_n (GPC) = 3.2 kDa, D = 1.10. ¹H NMR (400 MHz, CDCl₃) δ ppm 4.09 (q, J = 7 Hz, 2H), 2.37 – 2.09 (br, 22 H), 1.95 – 1.76 (br, 9 H), 1.74 – 1.18 (br, 239 H), 1.17 – 1.09 (br 5H). ¹³C NMR (101 MHz, CDCl₃) δ ppm 174.5- 174.0, 80.7 – 80.4, 40.8 – 40.1, 28.3 – 28.0.

Synthesis of Poly(*tert*-butyl acrylate)₂₂-*b*-polystyrene₁₄₁ (PtBA₂₂-*b*-PS₁₄₁) via ATRP

Styrene (500 eq, 20.75 g, 199.2 mmol), PtBA₂₂ (1 eq, 1.20 g, 398.9 μ mol), PMDETA (1.5 eq, 339 mg, 0.6 mmol) and anisole (10 mL) were loaded in a flame dried 50-mL Schlenk-flask equipped with a magnetic stir bar. The reaction flask was sealed with a rubber septum and the solution was degassed by three FPT cycles. The CuBr catalyst (1.7 eq, 100 mg, 0.7 mmol) was added to the frozen reaction mixture under nitrogen gas flow and two additional cycles of FPT were performed. The reaction vessel was then allowed to warm up to room temperature and became homogenous through stirring for 10 minutes. The polymerization started by placing the flask into a preheated oil bath (90 °C). Aliquots were collected periodically and analyzed by ¹H NMR spectroscopy to monitor the polymerization. As the expected monomer conversion was reached after 7 h, the polymerization was quenched by immersing the reaction flask into liquid nitrogen and exposure to air. After evaporation of anisole, 50 mL THF was added to the reaction mixture and the catalyst was removed by filtering through a neutral alumina plug. The resulting product was purified by precipitation into cold methanol (2 \times). The precipitates were dried overnight under high vacuum on the Schlenk line to afford 4.81 g of PtBA₂₂-*b*-PS₁₄₁ as a white solid, giving 85% yield of the 25% monomer conversion. M_n (NMR) = 17.7 kDa, M_n (GPC) = 22.0 kDa, D = 1.12. FTIR: 3109 – 2793, 1728, 1597, 1489, 1450, 1366, 1250, 1150, 1026, 903, 841, 756, 694 cm⁻¹. ¹H NMR (400 MHz, CDCl₃) δ ppm 7.23 – 6.88 (br, 424H) 6.87 – 6.23 (br, 281H) 4.09 (q, J = 7 Hz, 2H), 2.34 – 2.14 (br, 22H), 2.13 – 1.08 (br, 695H). ¹³C NMR (101 MHz, CDCl₃) δ ppm 128.3 – 128.0, 127.9 – 127.6, 125.9 – 125.5, 77.4, 40.8 – 40.1, 28.4 – 28.0.

Synthesis of Poly(acrylic acid)₂₂-*b*-polystyrene₁₄₁ (PAA₂₂-*b*-PS₁₄₁)

In a round bottom flask PtBA₂₂-*b*-PS₁₄₁ (1.50 g, 84.9 μmol) was dissolved in dichloromethane (40 mL). The reaction mixture was stirred after the addition of an excess amount of TFA (9 mL, 0.1 mol). After 16 h, the solvent and TFA were evaporated by blowing air into the reaction flask. The resulting solid was dissolved in THF and transferred into a presoaked dialysis tubing (6-8 MWCO) and dialyzed against nanopure water for 2 days. During dialysis, some early precipitation happened. The precipitates along with the solution were lyophilized to yield a white powder. FTIR: 3642 – 2137, 1828 – 1558, 1489, 1450, 1366, 1211, 1165, 1065, 1026, 903, 841, 756, 694 cm^{-1} . ¹H NMR (400 MHz, d₈-THF) δ ppm 10.83 (br, 5H), 7.32 – 6.80 (br, 489H) 6.80 – 6.26 (br, 300H), 4.04 (q, $J = 7$ Hz, 2H), 2.25 – 2.08 (br), 2.09 – 1.05 (br, 883H). ¹³C NMR (101 MHz, d₈-THF) δ ppm 145, 135.7, 129.2 – 128.3, 126.8 – 126.3, 68.2 – 67.6, 41.7, 30.9, 26.1 – 25.2.

SEC traces showed that the initial PtBA₂₂ homopolymer and the subsequent PtBA₂₂-*b*-PS₁₄₁ diblock copolymer were monomodal with narrow dispersity (Figure II.1). Scheme II.1 summarizes the synthesis steps of PAA₂₂-*b*-PS₁₄₁.

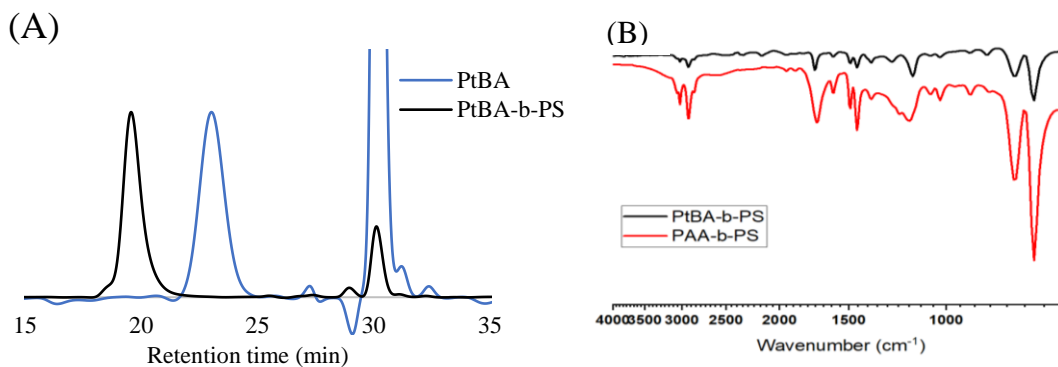
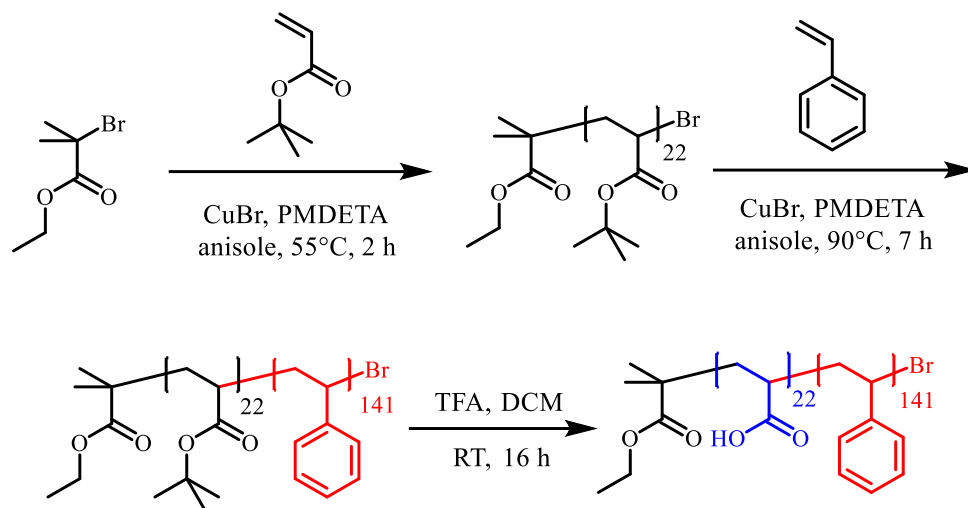


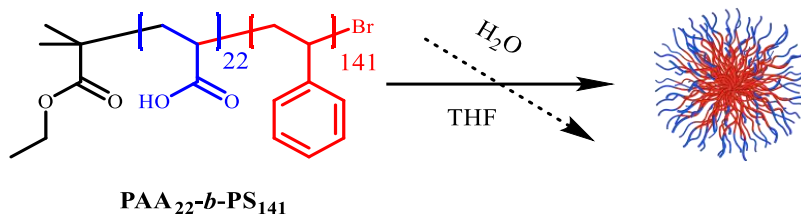
Figure II.1 (A) SEC traces of PtBA₂₂ in blue and PtBA₂₂-*b*-PS₁₄₁ in black (B) IR spectra of PtBA-*b*-PS in black and PAA-*b*-PS in red



Scheme II.1 Synthesis of the amphiphilic diblock copolymer of PAA₂₂-*b*-PS₁₄₁

Preparation of PAA₂₂-*b*-PS₁₄₁ micelles

In a 500-mL round bottom flask, PAA₂₂-*b*-PS₁₄₁ (375 mg) was dissolved in 75 mL THF and was stirred for 10 min. Nanopure water (75 ml) was added dropwise via a syringe pump at a rate of 20 mL/h to obtain a nanoparticles solution with the concentration of 2.5 mg/mL in 50% THF in water (Scheme II.2) Organic solvent removal of the resulting nanoparticles solution was obtained by excessive dialysis using tangential flow filtration (diafiltration system) or batch dialysis.



Scheme II.2 Schematic representation of solution-state self-assembly of PAA-*b*-PS into micelles

Diafiltration System (DFS) Experimental Setup

A common TFF system is composed of a buffer addition system, feed tank, feed pump, filtration module, pressure gauges, needle valve to control the pressure, and, tubing to connect different system parts. Figure II-4 (A) demonstrates a schematic of the experimental setup alongside a picture of the designed TFF system.

The PAA-*b*-PS assemblies in 50% THF in water were loaded into the feed tank under constant mixing using a magnetic stir bar (Figure II-4 (B)). A peristaltic pump was used to pump the solution from the feed tank to the membrane cassette. The pump was operated at a constant flow rate throughout all experiments. The pressure on the feed line was monitored using a pressure gauge. The feed was pumped into a Pellicon 3 cassette with Ultracel (composite regenerated cellulose) membrane with nominal molecular weight cutoff (MWCO) of 10 kDa (regenerated cellulose has fair chemical resistance to most organic solvents including tetrahydrofuran). Another pressure gauge was attached to the retentate outlet, followed by a needle valve. The needle valve was used to limit the effective cross area that the flow could pass through and therefore the creation of backpressure. By adjusting the needle valve, one could control the retentate pressure and affect the feed pressure resulting in increasing or decreasing of transmembrane pressure (TMP). A three-way valve was connected to the retentate line in order to facilitate sampling during diafiltration. The retentate line was directed back into feed tank to create a closed-loop. In continuous diafiltration, buffer should be added to the feed tank at the same rate as the filtrate leaves the system. In order to achieve this, the permeate (filtrate) flow rate was constantly tracked and recorded through continuous mass measurement of

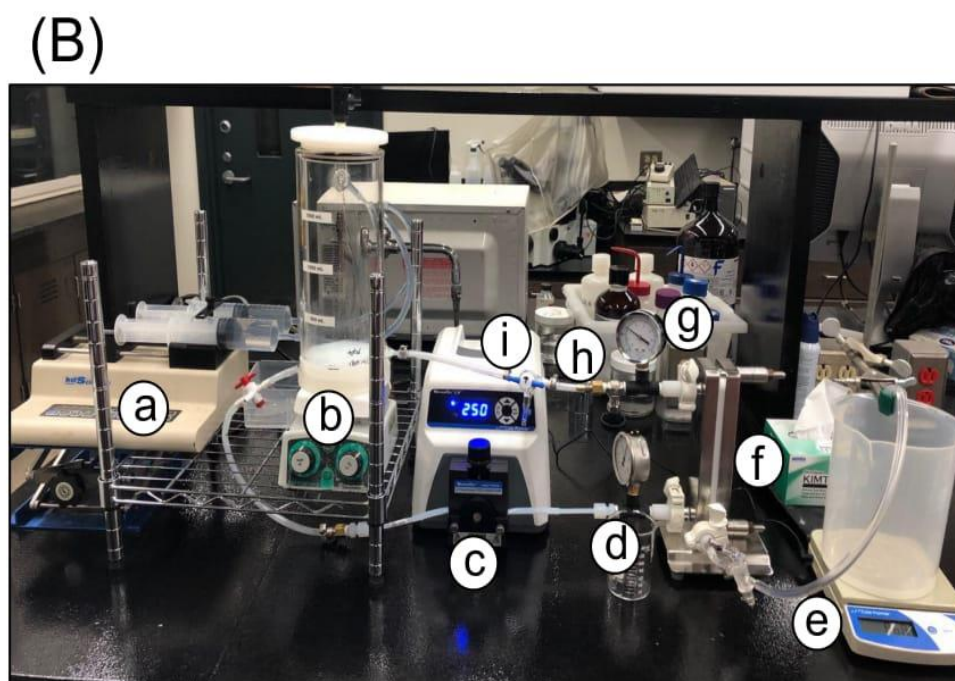
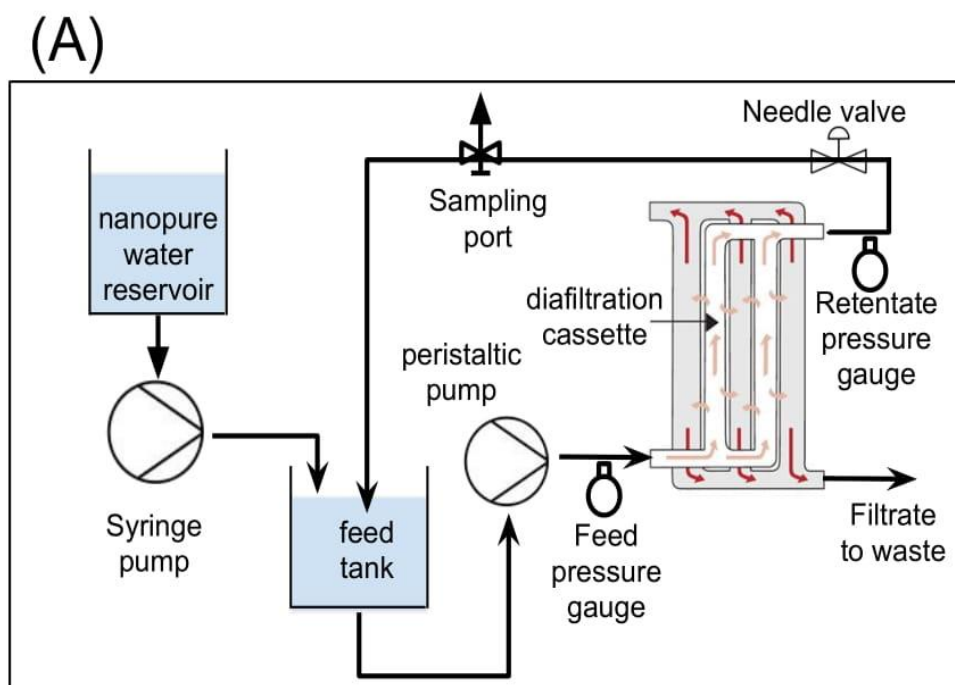


Figure II.2 (A) Schematic of the experimental setup. (B) Picture of the diafiltration system which consists of (a) syringe pump for buffer addition, (b) feed tank, (c) peristaltic pump, (d) feed pressure gauge, (e) permeate flow rate measurement scale, (f) cassette holder and cassette, (g) retentate pressure gauge, (h) needle valve for pressure regulation, and (i) sampling port.

the permeate flow on a weighing scale. The calculated permeate flow rate was used to set the syringe pump flow rate that added the buffer (nanopure water) to the feed tank. In addition, the volume of the fluid in the feed tank was visually checked to ensure a constant amount of fluid in the system throughout the experiment.

Chemical compatibility of all wetting parts with the solvent is crucially important. Here, a custom 2-liter glass feed reservoir was fabricated, which was compatible with THF. The only compatible peristaltic pump tubing commercially available was made from polytetrafluoroethylene (PTFE), which is a rigid material. Due to this challenge, a special kind of pump head (PTFE compatible) was used to ensure reliable flow rate. All other tubing had chemically compatible fluorinated ethylene propylene (FEP) lining on the wetting side. All valves and connections were made from compatible polyvinylidene fluoride (PVDF), nylon, brass, stainless steel, or glass. Another consideration was the pressure rating of the system, which was above 70 psig for all the pressurized components of the system.

Initial Setup and Pump Calibration

Prior to the usage of the membrane for diafiltration experiment, some initial calibration and preparation steps were required. First, pump calibration test was performed. The precision variable-speed pump drive was used with a PTFE pump head. The pump speed reading in unit of round per minute (RPM) was converted to flow rate (mL/min). For the calibration test, the feed tank was loaded with nanopure water, which was pumped using the peristaltic pump into a tared container on a weighing scale. The

pump speed was set to 9 different RPM values between 10-300 RPM, mass reading was recorded after one minute and this measurement was repeated 3 times for each pump speed to decrease the measurement error. The equation, $Q_F \text{ [mL/min]} = 0.1657 \times \text{pump speed [RPM]} - 1.102$ was used for converting pump speed to flow rate.

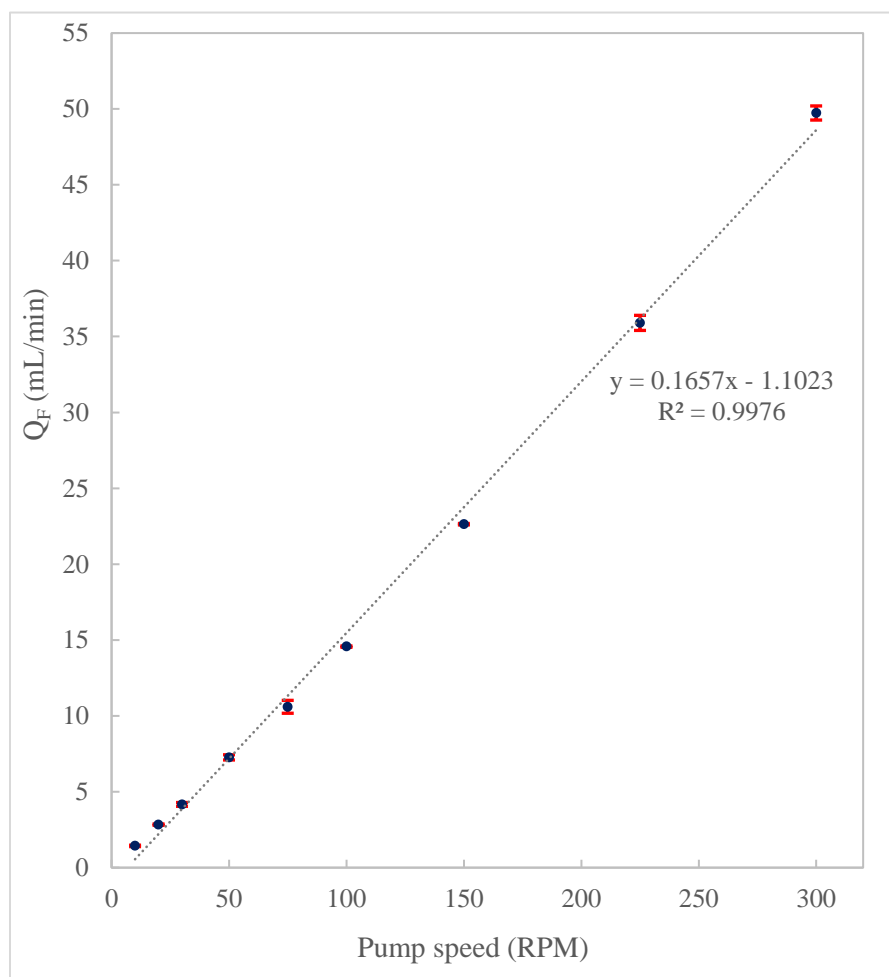


Figure II.3 Pump calibration measurements with error bar at each data point shown in red.

Cleaning of the Membrane Cassette

The Pellicon membrane cassettes are usually stored in a preservative solution of 3-4% benzyl alcohol, 20% glycerin and water before shipping. The storage solution was flushed out with water and 0.2 N sodium hydroxide solution at a feed flow rate of 44 mL/min equal to 5 L/min/m² of membrane area within the range recommended by the manufacturer (4-6 L/min/m²). The NaOH solution was recirculated through the system for 30 minutes and then flushed out with enough nanopure water, until neutral pH was achieved on both permeate and retentate lines.

Measurement of Water Permeability

The normalized water permeability (NWP) of the membrane was measured to establish a baseline that one would use to ensure membrane cleanness before reusing. Retentate pressure was set at 6 psig using the needle valve, the pump rate was set at a value (\approx 200 RPM) that resulted in a feed pressure of 10 psig with nanopure water as the fluid. The permeate flow rate was measured to calculate the cross-membrane flux rate. Finally, NWP was calculated using Equations 1 and 2.

$$\text{NWP} \left[\frac{\text{L}}{\text{m}^2 \cdot \text{h} \cdot \text{psi}} \right] = \frac{\text{flux rate} \left[\frac{\text{L}}{\text{m}^2 \cdot \text{h}} \right]}{\text{TMP} [\text{psig}]} \quad (\text{Equation 1})$$

$$\text{TMP} = \frac{P_{\text{Feed}} + P_{\text{Retentate}}}{2} \quad (\text{Equation 2})$$

Preparation of DFS for Diafiltration Experiment

Another step before running any diafiltration experiment is measuring the holdup volume of the system. This is the volume of fluids present only in the tubing and the cassette. Holdup volume should be considered for calculating the total system volume. To measure the holdup volume first, the water level in the feed tank was decreased to the minimum working volume (the least amount of liquid required in the feed tank before the air enters the line). Then the permeate valve was closed and all the fluid in the system was pumped out and collected into a tared vessel through the sampling port. The system holdup volume was calculated from the mass of the collected water plus the membrane holdup volume, which is 5 mL for the cassette used. The holdup volume of the demonstrated setup was 30 mL.

A common term used in the diafiltration process is diafiltration volumes or diavolumes, which is a measure of extent of washing performed during diafiltration (Equation 3). In a constant concentration diafiltration the process volume is constant, and the water is introduced to the system at the same rate that permeate leaves.

$$N_D = \frac{V_{\text{water}}}{V_{\text{process}}} \quad (\text{Equation 3})$$

N_D : Number of diavolume

V_{water} : Volume of fresh water added

V_{process} : Process volume

The nanopure water used in the experiments was made basic (pH = 8) by addition of NaOH to it. This modification was made following some unsuccessful experiment with nanopure water at a pH of 4.5.

Transmembrane Pressure Optimization

Using DFS, nanoparticles of PAA-*b*-PS were diafiltered at different initial concentrations of 1.0, 2.5, and 4.0 mg/mL while the concentration was maintained constant during the experiments. It has been reported that the filtrate flux rate increases with increasing the TMP and then it reaches a plateau as demonstrated in TMP excursion plot (Figure II. 4A).⁵¹ The first part of the curve is in a pressure-dependent regime, where permeate flux rate increases with transmembrane pressure and the limiting factor for flux is the fouled membrane resistance. The plateau part or the pressure-independent regime occurs when further pressure increases result in constant permeate flux. The transition point between these regions is called a “knee” and is the optimal point to perform ultrafiltration experiment. At the knee point, the permeate flux is maximized while pressure-driven membrane fouling is minimized.

In our experiments, at a constant feed flow rate, the retentate pressure was elevated from 0 and 20 psig to determine the knee point. The TMP excursion was plotted using the recorded permeate flux and the pressure on feed and retentate lines. However, this optimal pressure point was not achieved. In most experiments, the difference between the feed pressure and the retentate pressure (ΔP) was relatively high (in the range of 10 to 35 psig). Therefore, further increase of the retentate pressure imposed high pressure on the feed line to a point that the feed pressure became very unstable and the continuation of the TMP optimization experiment was unfeasible due to pressure limitations of the system.

Although TMP excursion was performed for all experiment, the DFS was operated at a constant retentate pressure of 20 psig during most of the diafiltration experiments.

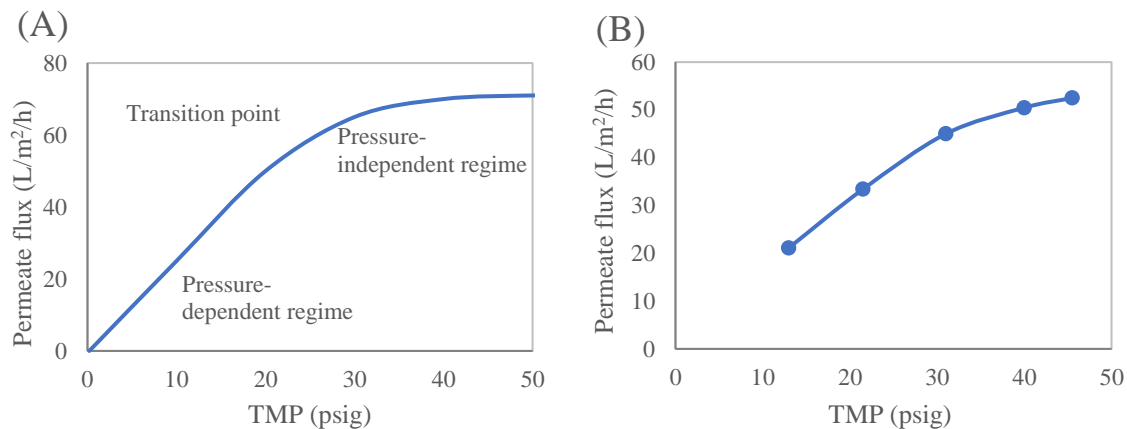


Figure II.4 (A) An example of TMP excursion plot (B) TMP excursion plot for diafiltration experiment of PAA_{47-b}- PS₂₃₅ nanoparticles

THF Measurements using HSGC

Solvent content (THF:water) of the samples were measured using gas chromatography-mass spectrometry (GC-MS). The GC was equipped with a headspace gas chromatography (HSGC) autosampler, which extracted an aliquot of headspace vapors of the vial and injected it to the GC column. The vial was equilibrated at 70 °C for a set period of time, which resulted in the migration of more volatile species (THF) from the liquid phase of the sample to the gas phase.

Standard solutions with THF content of 0.1 %, 0.08 %, 0.04 %, 0.02%, 0.01 %, 0.005 %, 0.001 % (by volume) in water were prepared. The standard solutions were analyzed by HSGC and a calibration curve was plotted (Figure II.5). The quantification range with a linear relationship between peak area and THF content was identified to be 0.001% to 0.08% of THF in water (by volume).

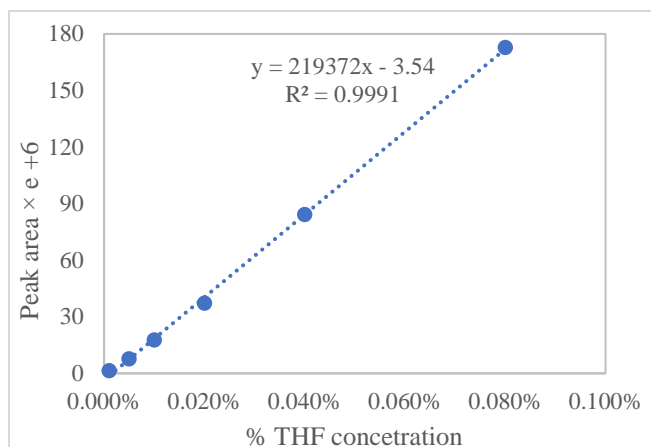


Figure II.5 HSGC calibration curve

The following method was implemented on GC-MS for THF analysis. The initial oven temperature was 30 °C (with 2 minutes hold time), which was ramped up at a rate of 40 °C/min until 100 °C was reached. The agitator was set to 70 °C with a sample incubation time of 2 minutes. The injection speed into vial was set to 40 mm/s and the syringe temperature was 80 °C. Data acquisition was started after 1.5 minutes to avoid oxygen damage to the filament. Scan mode was set to single ion monitoring with the defined molar mass of THF. The split ratio of 1:100 was applied to all samples.

Sample preparation for HSGC

Nanoparticles solution samples were diluted so that the approximate THF content fell in the quantification range. Samples with an expected higher concentration of THF were diluted 700, 600, or, 500 times, while the samples with lower expected THF content were prepared with a dilution factor of 400, 300, and in some cases 100. For sample preparation with dilution factor of 500, 4.99 mL of nanopure water and 10 µL of sample were added to a vial using proper micropipettes, followed by proper mixing. Subsequently,

2 mL of the fluid was transferred into a 20 mL HSGC vial. The vial was sealed using appropriate septum and aluminum clamp to avoid evaporation.

Hydrodynamic Size Measurement using DLS

The collected samples during diafiltration experiments were characterized by DLS to determine their hydrodynamic particle size. DLS measurements were conducted on a Zetasizer Nano ZS instrument, which allows for modification of dispersant after the acquisition of measurement results. The average number hydrodynamic diameter of nanoparticles was reported in the results and discussion chapter.

Analysis of THF content in each sample was used to revise the viscosity, refractive index (RI) and dielectric constant (ϵ) of the dispersant. The viscosity, RI and dielectric constant in a binary mixture of THF and water were calculated based on the mole fraction of THF and water.^{52, 53}

Experimental Design

A total of nine experiments were conducted to examine the effect of change of transmembrane pressure, nanoparticle concentration, and hydrophobic/hydrophilic block ratio on solvent exchange and nanoparticle size evolution during the TFF process. Table II.1 shows a list of the TFF experiments with their corresponding experimental conditions. In addition, three batch dialysis experiments were performed to compare TFF purification with purification in a batch setting using dialysis.

A baseline experiment was performed to examine the solvent exchange process in the lack of nanoparticles using a 50% solution of THF in nanopure water. To study the effect of change of transmembrane pressure on solvent exchange two experiments were carried out using the same polymeric nanoparticles (PAA₄₇-*b*-PS₂₃₅) with 1.0 mg/mL concentration at retentate pressures of 10 psi and 20 psi. To determine whether or not the diafiltration process depends on the concentration of the nanoparticles in the suspension, three experiments were performed using PAA₆₄-*b*-PS₆₀ at the retentate pressure of 20 psi with concentrations of 1.0, 2.5, and 4.0 mg/mL. Two sets of experiments were used to analyze the effect of change of PS/PAA block ratio at two different concentrations. In the C1 set shown in Table II.1, polymeric nanoparticle solutions with block ratios of ≈ 1.0 , 2.0, and 5.0 were tested at the constant concentration of 1.0 mg/mL under retentate pressure of 20 psi. Similarly, three different experiments were performed at the higher concentration of 2.5 mg/mL (Table II.1 set C2.5).

In addition, three batch dialysis experiments with PAA₆₄-*b*-PS₆₀, PAA₈₅-*b*-PS₁₈₂, and PAA₄₇-*b*-PS₂₃₅ were conducted to evaluate the effect of using in-flow TFF (Table II.1 set B) compared to the traditional batch dialysis in terms of duration of experiments and evolution of hydrodynamic diameter of particles (data is shown in Appendix A).

Table II.1 Performed experiments to study the effect of transmembrane pressure (A), PS/PAA block ratio (C1, C2.5), and nanoparticles concentration (D) on the TFF process. In addition, (B) experiments were compared to batch dialysis experiments.

Solution	Average P _F (psig)	Average P _R (psig)	Average TMP (psig)	Solid content (mg/mL)	Intended purpose
50% THF	42.0	38.0	40.0	-----	
PAA ₄₇ - <i>b</i> -PS ₂₃₅	22.0	10.0	16.0	1.0	A
PAA ₄₇ - <i>b</i> -PS ₂₃₅	32.0	20.0	26.0	1.0	A, C1
PAA ₆₄ - <i>b</i> -PS ₆₀	46.0	20.0	33.0	2.5	B, D, C2.5
PAA ₆₄ - <i>b</i> -PS ₆₀	42.0	20.0	31.0	1.0	D, C1
PAA ₈₅ - <i>b</i> -PS ₁₈₂	36.0	20.0	28.0	1.0	B, C1
PAA ₆₄ - <i>b</i> -PS ₆₀	56.0	20.0	38.0	4.0	D
PAA ₄₇ - <i>b</i> -PS ₂₃₅	56.0	20.0	38.0	2.5	B, C2.5
PAA ₂₂ - <i>b</i> -PS ₁₄₁	46.0	20.0	33.0	2.5	C2.5

CHAPTER III

RESULTS AND DISCUSSION

Feasibility of incorporating an in-flow diafiltration system to scale-up the purification step of the synthesis of PAA-*b*-PS polymeric nanoparticle was explored using a custom-built tangential flow filtration (TFF) setup. Residual organic solvent contents and diameters of nanoparticles were measured and analyzed throughout the experiments. Batch dialysis experiments were performed to contrast with the in-flow solvent exchange system and to understand the possible extent of scale-up using the TFF. In addition, the effects of change of transmembrane pressure, nanoparticles concentration, and hydrophobic/hydrophilic block ratio on the solvent exchange process were studied.

In-flow Purification of Block Copolymers Assemblies using TFF

Feasibility of using the proposed setup for purification of solutions of amphiphilic block copolymers assemblies was examined through comparison of two nanoparticles solutions purification experiments with a baseline experiment, in which a 50:50 THF:water solution (without nanoparticles) was purified.

Two experiments with PAA₆₄-*b*-PS₆₀ and PAA₄₇-*b*-PS₂₃₅ nanoparticles were prepared by solution self-assembly as previously described. In each experiment, approximately 140 mL of the nano-assemblies solution with a concentration of 2.5 mg/mL (0.25 wt%) in a 50:50 THF:water solution was used as the feed solution. Since the holdup volume of the system was 30 mL, the initial process volume was 170 mL. The feed was

circulated in the DFS to uniformly mix the nanoparticles solution with the holdup fluid. Subsequently, a 20 mL sample was taken out using a syringe to make the final process volume 150 mL. The concentration values mentioned in this chapter are normally the concentration before the addition of nanoparticles into the feed tank, right after assembly. Similarly, the process volume of the baseline (50% THF) experiment was 150 mL. Nanopure water with pH of 8.0 was used as the dilution buffer. Transmembrane pressure was maintained around 40 psig (pounds per square inch gauge) in the baseline experiment while the average TMP for the nanoparticles suspensions experiments were 33 and 38 psig.

The average permeate flow rate during purification of the 50 % THF solution without nanoparticles was 26 mL/min, a much higher value compared to the average permeate flow rates of 14 mL/min in both nanoparticle experiments. Therefore, the presence of nanoparticles extended the solvent exchange process as the addition of buffer had to be slower.

Figure III.1A demonstrates a comparison of change of relative THF concentration (sample concentration divided by initial concentration) over time among these experiments. The relative concentration was used instead of the absolute concentration to remove the effect of small variations of initial concentrations on the plots. In addition, due to the inability of the Cartesian coordinates in showing changes over a wide range of values, the logarithm of the relative concentration (Figure III.1B) was also used to better distinguish the tail of the experiments. As shown in Figure III.1, six diavolumes of buffer had been added to the 50 % THF after only 35 minutes of diafiltration. However, only 2.5

diavolumes had been added to the solutions of nanoparticles in the same time span. After 35 minutes, the THF content had dropped to roughly 2.0% of its initial value for the baseline experiment, while the corresponding level was around 8.0 % for the nanoparticle solutions. This was probably because of the formation of a thin cake of nanoparticles on the surface of the membrane, which could reduce the membrane permeability and possibly plug some membrane pores resulting in slower solvent exchange. Most importantly, purification of amphiphilic block copolymers assemblies in solutions containing aggressive organic solvents was demonstrated to be feasible using the proposed TFF setup.

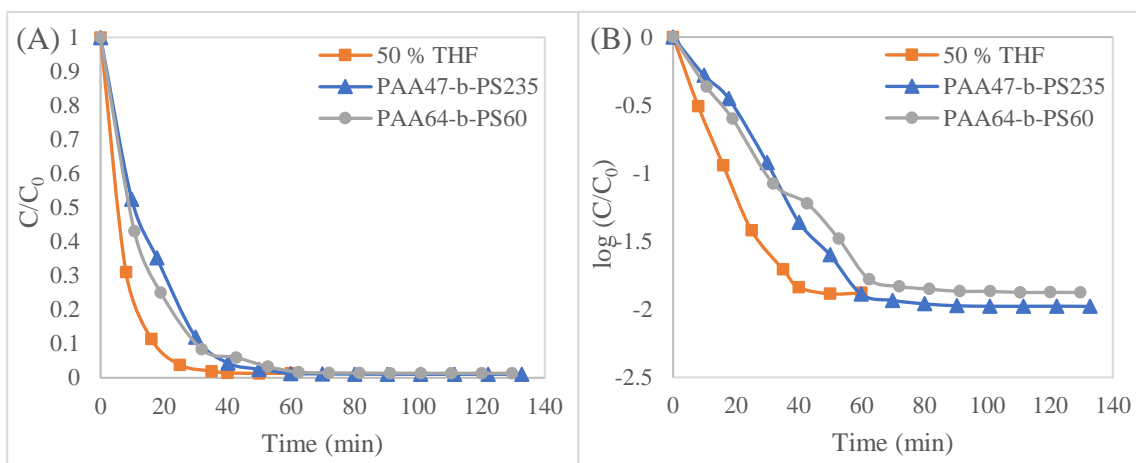


Figure III.1 Solvent exchange in 50% THF solution without nanoparticles is much faster solutions with nanoparticles (PAA₆₄-b-PS₆₀ and PAA₄₇-b-PS₂₃₅). (A) Absolute and (B) logarithmic relative concentration (sample THF concentration/initial THF concentration).

Tangential Flow Filtration vs. Batch Dialysis

Three batch dialysis experiments were designed to facilitate comparison of batch dialysis with diafiltration using the TFF system in terms of scale and effectiveness. Batch dialysis experiments were carried out using presoaked dialysis regenerated cellulose membrane tubing with 6-8 kDa MWCO. Dialysis was continued for 30 hours against 4 liters of nanopure water with pH of 8.0. The water was changed 5 times on the first day and twice on the second day. The solution was sampling (≈ 1 mL) with closer time interval at the beginning of the experiments (3h, 6h, 9h, and 12 h) followed by only two samples after that (22 h and 30 h). On average, 15 mL solution of polymeric assemblies were dialyzed in the batch experiments, which was only 10 % of the process volume used in TFF experiments at 150 mL.

Figure III.2 demonstrates evolution of relative THF concentration (absolute and logarithmic) during purification of nanoparticles solutions of PAA₈₅-*b*-PS₁₈₂ (1.0 mg/mL), PAA₆₄-*b*-PS₆₀ (2.5 mg/mL), and PAA₄₇-*b*-PS₂₃₅ (2.5 mg/mL) using TFF and traditional dialysis. In TFF experiments, the THF concentration reached the minimum level after 1 hour of in-flow filtration, while it took around 6 hours to reach similar levels of THF concentration in the batch setting. In addition to an order of magnitude difference between the processing volumes of TFF and dialysis, further scale-up of the TFF process is easily achievable with increasing the membrane area through utilizing larger membranes or by adding more membrane cassettes in the flow line.

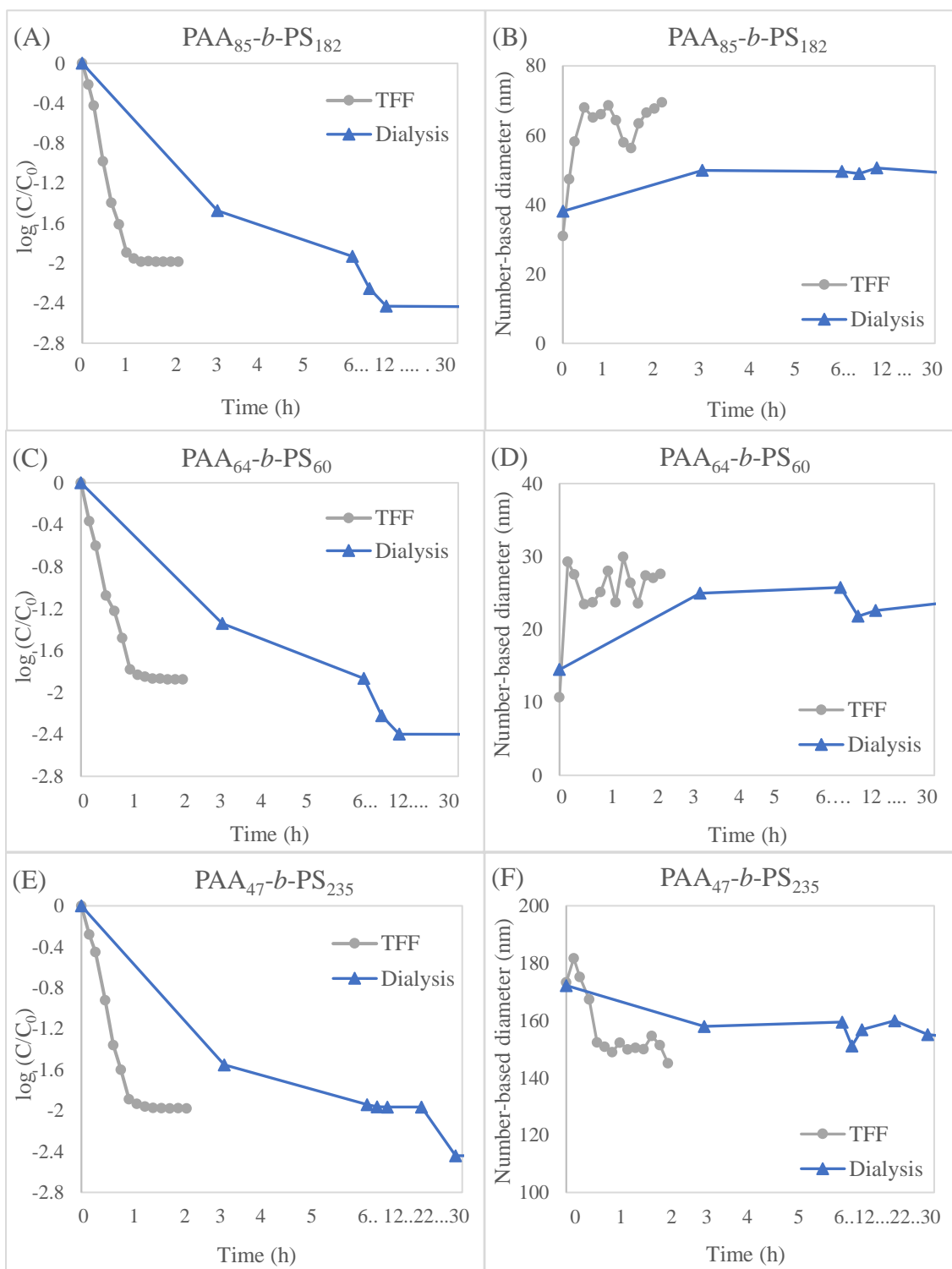


Figure III.2 Comparison of tangential flow filtration and traditional batch dialysis for purification of nanoparticles solution in 50:50 THF:water solution based on (A,C,E) logarithm of relative residual THF concentration and (B,D,F) changes of number-averaged diameter of nanoparticles over time.

The size evolution of nanoparticles during the experiments was also analyzed (Figure III.2 B, D, F). Nanoparticles in PAA₈₅-*b*-PS₁₈₂, PAA₆₄-*b*-PS₆₀ solutions had larger average number-based diameters using TFF compared to the traditional dialysis. However, the differences can be negligible when the standard deviations of diameter measurements are considered. The standard deviation of diameters for both in-flow and batch purification of PAA₆₄-*b*-PS₆₀ solutions is 8.0 nm, while it is around 15 nm for PAA₈₅-*b*-PS₁₈₂ solution. Self-assembly of PAA₄₇-*b*-PS₂₃₅ polymer has formed nanoparticles with number-averaged diameter of $\approx 155 \pm 46.0$ nm, which is significantly higher than the values expected for micelles. Unfortunately, DLS measurements are not sufficient to confirm the morphology of these assemblies. There is a high probability that these assemblies are either vesicles, rods, or large-compound micelles, which could be determined by a combination of atomic force microscopy (AFM), transmission electron microscopy (TEM), and DLS. The measurements are similar between TFF samples and the batch dialysis ones.

Effects of Transmembrane Pressure on TFF

Previous studies have explored the effect of transmembrane pressure (TMP) on the TFF process. Generally, the increase in pressure has expedited the solvent exchange process while in the pressure-dependent region. However, it has been reported that the separation speed reaches a plateau with the increase of the pressure beyond the pressure-dependent region.^{51, 54}

Here, two experiments were designed to evaluate the effect of pressure on the required time for completion of in-flow solvent exchange. Two 150 mL samples of PAA₄₇-*b*-PS₂₃₅ nanoparticles (in 50:50 THF:water solution) with a concentration of 1.0 mg/mL were obtained through the previously described in-solution self-assembly. Similar to previous experiments, nanopure water with an approximate pH of 8.0 was used as the dilution buffer.

In the first diafiltration experiment, retentate pressure was kept at 10.0 psig which resulted in an average feed pressure of 22.0 psig. Therefore, the mean transmembrane pressure (TMP) during the experiment was 16.0 psig. In the second experiment, the retentate pressure was increased to 20.0 psig, which resulted in transmembrane pressure of 26.0 psig. The TMP increase resulted in a substantial increase in the average permeate flow rate, which determined the buffer addition rate to the feed tank. Mean permeate flow rate was 9.7 mL/min with retentate pressure of 10.0 psig compared to 14.6 mL/min with retentate pressure of 20.0 psig. The experiments were continued to reach at least 1500 mL (10 diavolumes) of collected filtrate fluid.

The solvent exchange rate was directly proportional to the applied TMP across the membrane. As the TMP increased, the permeate flow rate increased, which resulted in faster purification. Figure III.3 verifies that the solvent exchange was significantly higher in the experiment with TMP of 26.0 psig compared to the one with 16.0 psig. As it can be seen in Figure III.3B, the experiment with TMP of 26.0 psig required around 100 minutes to reach 2% of the initial THF concentration. However, 140 minutes were required to reach this level of purification at TMP=16.0 psig. The TMP in both experiments were in the

pressure-dependent region and further efforts to perform the experiments at higher pressures failed due to appearance of intermittent pressure pulses that exceeded the maximum working pressure of the system.

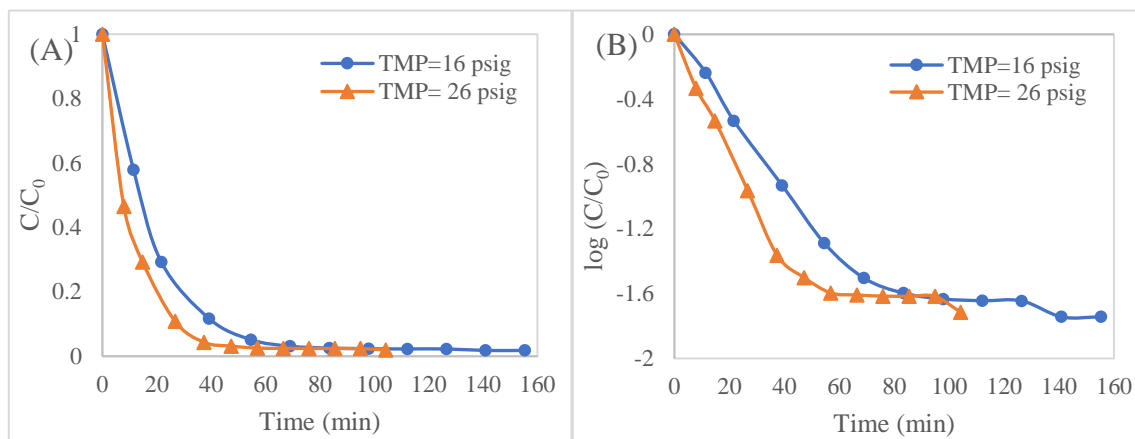


Figure III.3 Increasing TMP from 16 psig to 26 psig decrease the required time for diafiltration of PAA₄₇-*b*-PS₂₃₅ assemblies in 50% THF in water solution based on (A) absolute and (B) logarithmic relative concentration data.

In addition to THF concentration measurements, the diameters of nanoparticles were measured during the experiments. The measured differences between the two experiments were negligible. Figure III.4 demonstrates the evolution of particle diameters as a function of time. In both experiments, the number-averaged diameter was around 180 nm at the start of the experiment and increased to around 230 nm after addition of the first diavolume of water. However, with the continuation of the experiments, the diameter decreased and plateaued around 170 nm. The average standard deviation of all the samples in these experiments was approximately 50 nm. The diameters are larger than the expected value for micelles and suggest possible formation of vesicles, rods, or large-compound micelles.

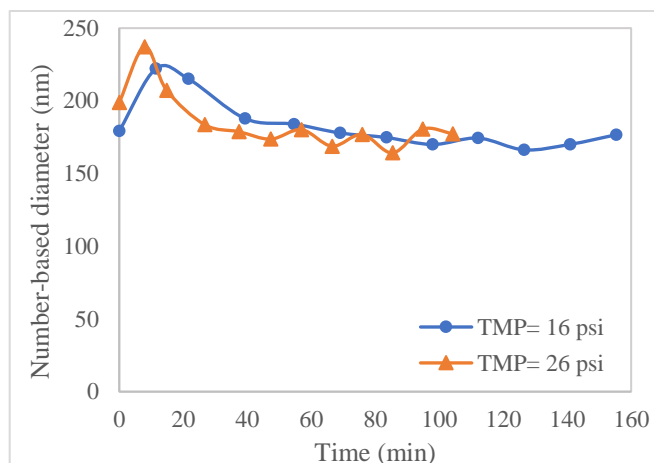


Figure III.4 Change of TMP has negligible effect on number-averaged diameter of PAA₄₇-*b*-PS₂₃₅ nanoparticles.

Effects of Initial Concentration of Nanoparticles on TFF

The effect of the concentration of nanoparticles in the suspensions on the diafiltration process was examined using three experiments with PAA₆₄-*b*-PS₆₀ assemblies and initial concentrations of 1.0, 2.5, and 4.0 mg/mL. The retentate pressure was kept constant at 20.0 psig through adjustment of the needle valve and the final system volume was 150 mL for all these experiments. The average TMP values of 30.7, 33.0, and 38.0 psig were obtained for the experiments with concentrations of 1.0, 2.5, and 4.0 mg/mL, respectively.

Figure III.5 shows that the TFF solvent exchange in solutions with concentrations of 2.5 and 4.0 mg/mL followed a similar trend. However, it took a significantly longer amount of time to reach the same levels of purification the experiment with 1.0 mg/mL concentration. Interestingly, feed pressure increased significantly during this experiment and forced us to decrease the feed flow rate (Q_F) at the beginning of the experiment to

prevent membrane fouling. Pressure significantly decreased after the first diavolume because of the decrease in THF concentration and the feed flow rate was increased to the desired initial 40 mL/min. The initial high pressure was unexpected since the concentration of nanoparticles in the solution was very low. The DLS particle diameter analysis shown in Figure III.6 revealed that at the start of the experiments, spheres in the 1.0 mg/mL solution were significantly smaller ($\approx 1.0\pm 0.2$ nm) compared to the spheres formed in the higher solid concentrations of 2.5 and 4.0 mg/mL ($\approx 10.0\pm 2.5$ nm). It is possible that the extremely small nanoparticles at 1.0 mg/ml had formed a more-packed cake on the surface of the membrane resulting in lower permeability and therefore, a higher difference in pressure. In addition, the smaller nanoparticles might have led to more clogging of the membrane pores.

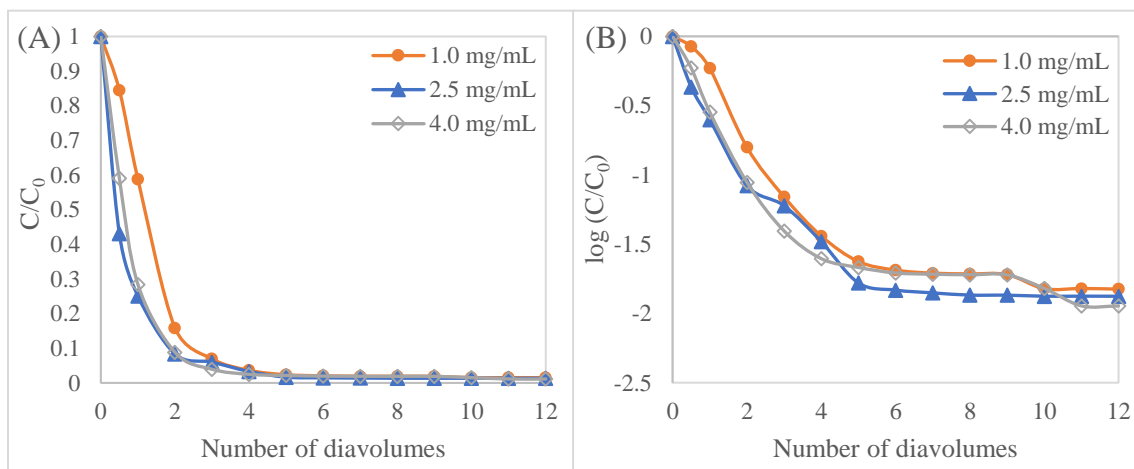


Figure III.5 Rate of organic solvent removal during diafiltration process of PAA₆₄-*b*-PS₆₀ assemblies was similar for solution with concentration of 2.5 mg/mL and 4.0 mg/mL and was slower for 1.0 mg/mL. (A) Absolute and (B) logarithmic relative concentration data.

The block copolymer micelles formed in the experiments with higher initial polymer concentrations were larger. Figure III.6 demonstrates the evolution of the number-averaged diameters of polymeric nanoparticles of PAA₆₄-*b*-PS₆₀ formed at different concentrations as a function of the added diavolumes of the buffer. The micelles diameters were around 10.0±2.5 nm for concentrations of 2.5 and 4.0 mg/mL at the start of the experiments. As the water addition continued, the diameter of micelles also increased. However, the diameter reached a steady-state around 27.0±6.0 nm after the first diavolume in the 2.5 mg/mL experiments while the diameter kept increasing till three diavolumes for the 4.0 mg/mL experiments when it reached 50.0±13.0 nm before the plateau. The diameter evolution for 1.0 mg/mL nanoparticles was more consistent with 2.5 mg/mL, with the exception that it started around 1.0 nm.

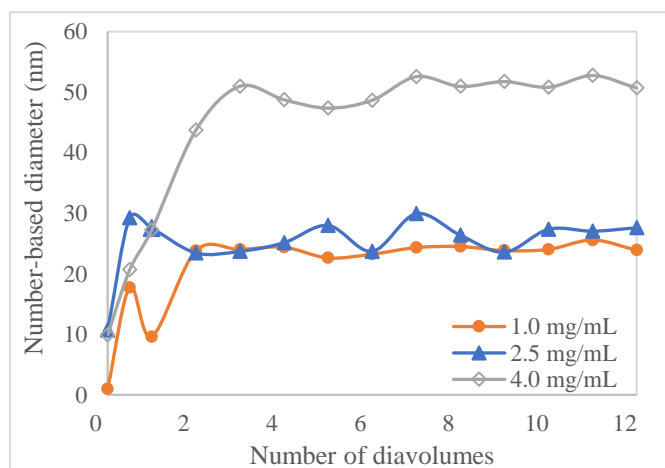


Figure III.6 The hydrodynamic size evolution for PAA₆₄-*b*-PS₆₀ assemblies with 1.0, 2.5 and 4.0 mg/mL initial polymer concentrations. Diameter of micelles formed in solution of 4.0 mg/mL concentration were almost double the ones with lower concentrations.

Our results agree with previous studies that have explored the effect of concentration of copolymers on the morphology and size of the resulting nanostructures. Zhang *et al.* showed that change of polymer concentration from 1.0 to 3.5 wt% (10 to 35 mg/mL) in PAA₂₀-*b*-PS₁₉₀ aggregates in dimethylformamide and water mixtures resulted in change of morphologies from spheres to rods and vesicles.⁵⁵ The aggregation number (N_{agg}), the average number of polymer chains in aggregate, is a function of polymer concentration $N_{\text{agg}} = 2 \sqrt{C/CMC}$, in which, C is the copolymer concentration and CMC represents the critical micellization concentration (copolymer concentration at the critical water content).⁵⁶ Aggregation number increases with increase of copolymer concentration, which results in formation of larger micelles cores.⁵⁶ This can explain the higher number-averaged micelles diameters observed at the higher initial copolymer concentration (4.0 mg/mL). Our results show that the initial nanoparticles concentration has a significant effect on the diameter of the formed structures during the TFF purification.

Effect of Block Ratio on TFF

Effect of Block Ratio on TFF at Concentration of 2.5 mg/mL

The effect of block ratio of the nanoparticles on the solvent exchange process was examined using six experiments at two different concentrations (2.5 mg/mL and 1.0 mg/mL). In the first set of experiments, three assemblies formed with the amphiphilic copolymers of PAA₄₇-*b*-PS₂₃₅, PAA₂₂-*b*-PS₁₄₁, and PAA₆₄-*b*-PS₆₀ at the initial concentration of 2.5 mg/mL were used. These polymers were chosen because of their wide range of sizes and block ratios, PAA₄₇-*b*-PS₂₃₅ ($M_{\text{n(NMR)}} = 28.0$ kDa, with hydrophobic to

hydrophilic ratio of 5.0), PAA₂₂-*b*-PS₁₄₁ ($M_{n(\text{NMR})} = 16.4$ kDa, with hydrophobic to hydrophilic ratio about ≈ 6.5) PAA₆₄-*b*-PS₆₀ ($M_{n(\text{NMR})} = 11.0$ kDa, with hydrophobic to hydrophilic ratio of about ≈ 1.0). The retentate pressure was maintained at 20.0 psig for all these experiments.

In most experiments, the tangential flow filtration was continued until 12 diavolumes of buffer had been added to the feed solutions to ensure achieving the highest possible extent of organic solvent removal. In this set of experiments, the diafiltration experiments for PAA₄₇-*b*-PS₂₃₅ and PAA₆₄-*b*-PS₆₀ followed this procedure. However, in the experiment with PAA₂₂-*b*-PS₁₄₁ nanoparticles, the experiment was stopped after the addition of only 6 diavolumes of buffer due to a sudden increase in feed pressure beyond the pressure rating of the system. Efforts for continuing the experiment through reduction of TMP via decreasing the feed flow rate and releasing the back-pressure on the retentate line were not successful in decreasing the pressure. Therefore, the product was recovered prematurely and the membrane and the DFS lines were washed according to the general washing procedure. Investigations revealed that the polymeric nanoparticles had precipitated inside the membrane-holder and possibly in the membrane and had caused clogging of pores, which resulted in the unusual pressure spikes. The precipitation might have happened due to the relatively higher ratio of hydrophobic to hydrophilic block in PAA₂₂-*b*-PS₁₄₁. Since solvent exchange occurs faster in TFF compared to batch dialysis, the accelerated increase of water to organic solvent ratio in the solution might have caused the nanoparticles to become insoluble and precipitate. Pictures of formation of solid precipitates on the inlet of the membrane holder are shown in Figure III.7.

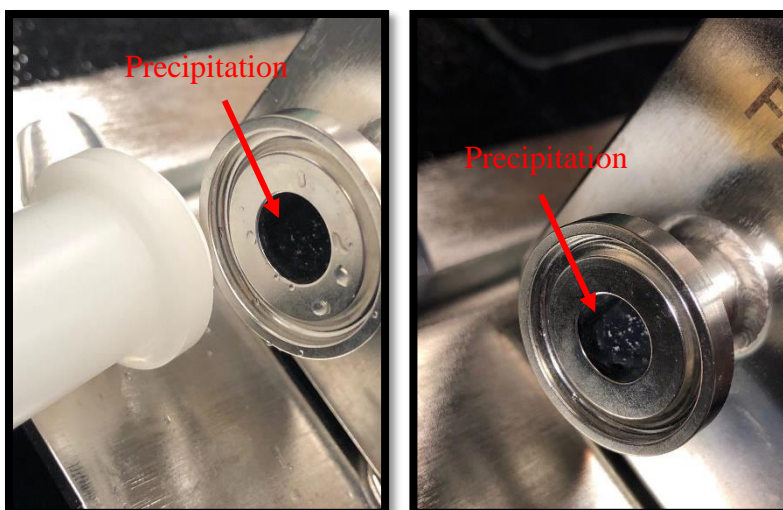


Figure III.7 Formation of precipitates at the feed inlet of the membrane holder.

Comparison of the relative THF concentration changes over time (Figure III.8) substantiates that THF removals from all solutions of nanoparticles follow a similar trend. Although only 6 diavolumes of buffer were added to the solution of PAA₂₂-*b*-PS₁₄₁, final THF content reached a very low level around 0.50 % of the initial THF concentration.

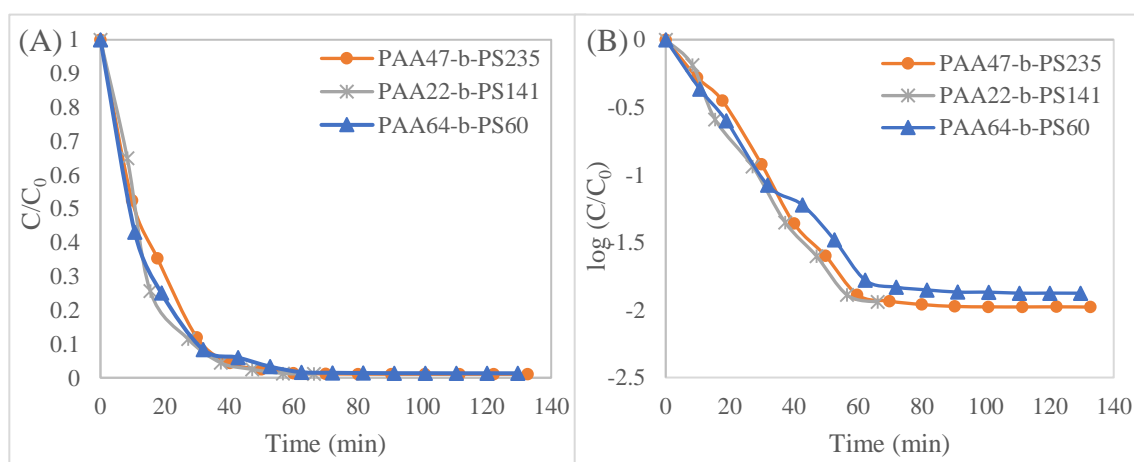


Figure III.8 Comparison of residual organic solvent content in the retentate samples collected from diafiltration process of different polymeric nanoparticles (PAA₆₄-*b*-PS₆₀, PAA₂₂-*b*-PS₁₄₁ and PAA₄₇-*b*-PS₂₃₅ with different block ratio at concentration of 2.5 mg/mL. (A) Absolute and (B) logarithmic relative concentration data.

Particle diameter plot (figure III.9) exhibits that the micelles formed from PAA₂₂-*b*-PS₁₄₁ and PAA₆₄-*b*-PS₆₀ had comparable number-averaged diameters of $\approx 20.0 \pm 5.0$ nm, and $\approx 27.0 \pm 6.0$ nm, respectively. However, in-solution assembly of PAA₄₇-*b*-PS₂₃₅ polymer has formed nanoparticles with number-averaged diameter of $\approx 155.0 \pm 46.0$ nm. Large nanoparticles diameter indicate the possible formation of vesicles, rods, or large-compound micelles in these assemblies.

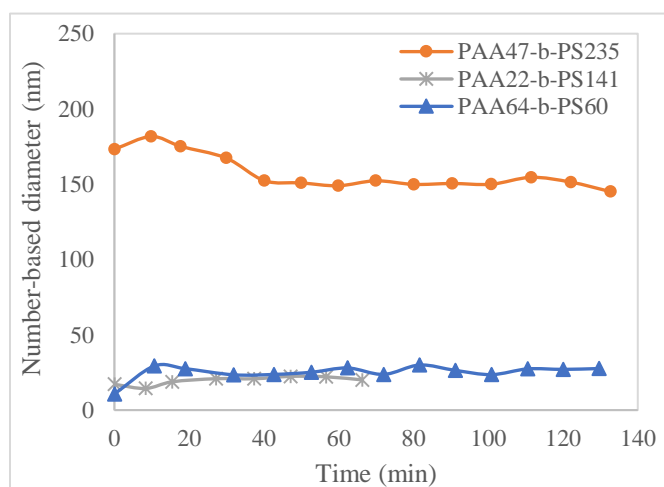


Figure III.9 The hydrodynamic size evolution of PAA₆₄-*b*-PS₆₀, PAA₄₇-*b*-PS₂₃₅, and PAA₂₂-*b*-PS₁₄₁ nanoparticles during TFF (conc.= 2.5 mg/mL).

Effect of Block Ratio on TFF at Concentration of 1.0 mg/mL

The second set of experiments were carried out using three block copolymers of PAA₄₇-*b*-PS₂₃₅, PAA₈₅-*b*-PS₁₈₂, and PAA₆₄-*b*-PS₆₀ at an initial concentration of 1.0mg/mL. The polymers had different sizes and block ratios, PAA₄₇-*b*-PS₂₃₅ ($M_{n(NMR)} = 28.0$ kDa, with hydrophobic to hydrophilic ratio of 5.0), PAA₈₅-*b*-PS₁₈₂ ($M_{n(NMR)} = 25.2$ kDa, with hydrophobic to hydrophilic ratio about ≈ 2.0) PAA₆₄-*b*-PS₆₀ ($M_{n(NMR)} = 11.0$ kDa, with hydrophobic to hydrophilic ratio of about ≈ 1.0)

Figure III.10 demonstrates a comparison of the relative THF concentration change as a function of time. In the logarithmic plot, Figure III.10B, PAA₈₅-*b*-PS₁₈₂ and PAA₄₇-*b*-PS₂₃₅ followed a similar behavior for about 40 minutes, when the THF concentration in both had declined to about 4% of their initial values. After this point, the trends start to differ due to unknown reasons. The results of the PAA₆₄-*b*-PS₆₀ experiment displayed a slower solvent exchange, which can be due to the significantly smaller size of the nanoparticles resulting in the formation of highly packed cake on the surface of the membrane and reduction of cross-membrane flow rate.

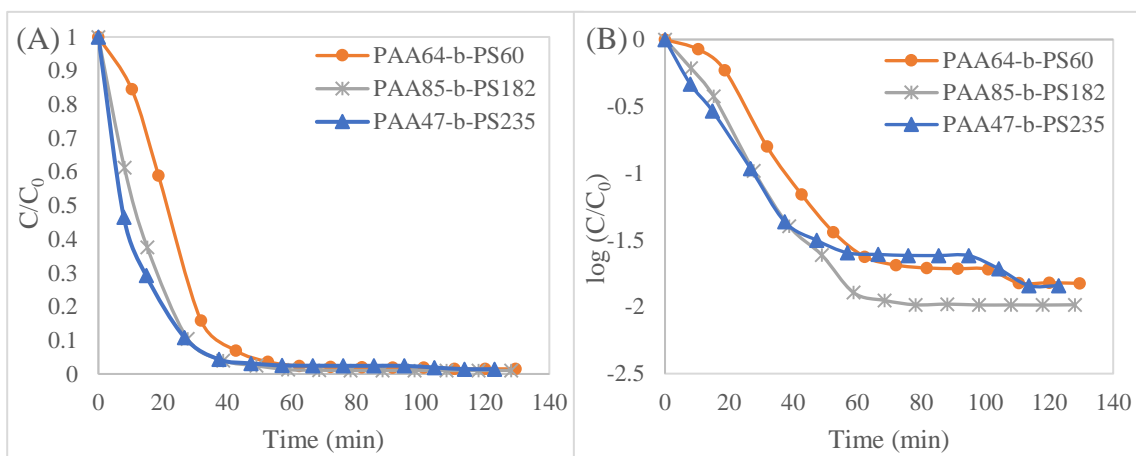


Figure III.10 Comparison of residual organic solvent in the retentate samples during purification of PAA₆₄-*b*-PS₆₀, PAA₈₅-*b*-PS₁₈₂ and PAA₄₇-*b*-PS₂₃₅ at concentration of 1.0 mg/mL. (A) Absolute and (B) logarithmic relative concentration data.

The evolutions of the number-averaged diameters of micelles formed in these experiments are shown in Figure III.11. As expected, spheres created from PAA₆₄-*b*-PS₆₀ block copolymers were the smallest followed by spheres of PAA₈₅-*b*-PS₁₈₂ block copolymers while the particles made from PAA₄₇-*b*-PS₂₃₅ were the largest ones. Interestingly, the diameters in the PAA₄₇-*b*-PS₂₃₅ experiment started $\approx 199.0 \pm 42.0$ nm and

then temporarily increased to $\approx 237.0 \pm 59.0$ nm. As the experiment went on, the number-averaged diameter decreased and remained steady around 180.0 ± 50.0 nm. The size of nanoparticles in this case slightly decreased during the transition from 50% organic solution to a fully aqueous system, which could be because of core deswelling as a result of THF removal. Micelles produced from PAA₈₅-*b*-PS₁₈₂ polymers started with a diameter of 31.0 ± 9.0 nm and ended up around 69.0 ± 20.0 nm after complete solvent exchange.

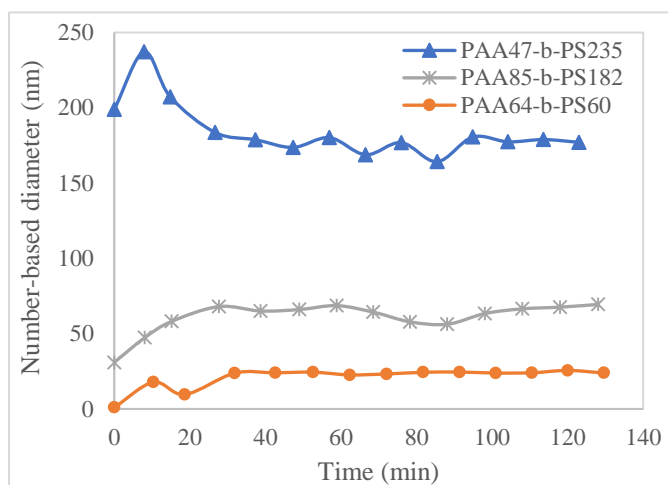


Figure III.11 The hydrodynamic size evolution of PAA₆₄-*b*-PS₆₀, PAA₄₇-*b*-PS₂₃₅, and PAA₈₅-*b*-PS₁₈₂ nanoparticles during TFF (conc.= 1.0 mg/mL)

Our results indicate that the efficiency of the solvent exchange process using TFF is probably independent of the block ratio of the nanoparticles used in the experiments. However, there might be an upper limit to the ratio of hydrophobic to hydrophilic blocks under which the system could perform without precipitation. To purify higher block ratio nanoparticles using the TFF system, one might be able to use membranes with smaller pore sizes to limit the buffer addition rate and alleviate the precipitation issue.

CHAPTER IV

CONCLUSIONS AND FUTURE WORK

Novel nanoparticles have been synthesized with promising potential for applications ranging from drug delivery to environmental remediation. However, many of these nanoparticles are synthesized at the laboratory scale. Fundamentally, the scaled-up production of nanotechnological materials is of importance in defining parameters and processes by which to achieve rapid fabrication with reproducibility.

Polymeric nanoparticles with amphiphilic core-shell morphologies have characteristics that result in their performance in a wide range of applications. A well-known class of nanomaterials with a core-shell morphology are shell cross-linked knedel-like nanoparticles,^{1, 2} which have received a lot of interest due to their well-defined structures and tunable physical and chemical functionalities.^{3, 4} A transition of organic polymers from a solvated state in an organic solvent to a dispersed phase in water occurs during solution-state supramolecular assembly of amphiphilic block polymers. However, conventional bulk processes for the preparation of such materials are impractical on large scales. As the most important conclusion of this work, it was shown that the use of an in-flow tangential flow filtration system to scale-up the solution-state transition during the synthesis of poly(acrylic acid)-*b*-polystyrene assemblies is feasible.

Purification of solutions with and without nanoparticles followed significantly different trends. The average transmembrane flow rate using a 50% THF solution (no nanoparticles) was almost twice the value in the presence of nanoparticle under

comparable transmembrane pressure. This was mainly due to the formation of a nanoparticle cake on the surface of the membrane, which decreased the overall membrane permeability. Purification with the TFF system was performed with considerably higher process volume compared to batch dialysis while significantly less volume of buffer was used. The in-flow process could be easily further scaled up (orders of magnitude) using membranes with a large surface area. In addition, the TFF purification decreased the organic solvent content considerably faster than batch dialysis. The organic solvent concentration reached its minimum level after 1 hour of diafiltration using TFF for a feed volume 10 times more than the solution in the batch dialysis. However, reaching the minimum level of organic solvent took around 6 hours in the batch setting. Therefore, tangential flow filtration showed to be a feasible approach with a high ceiling for scaled-up of solvent transition during the production of nanoparticles both in terms of higher possible processing volume and shorter required time.

Purification using TFF was found to be a resilient process with respect to operational conditions and parameters such as the applied pressure, initial nanoparticles concentration, and hydrophobic/hydrophilic block ratio. In general, change of transmembrane pressure and initial concentration of polymer assemblies affected the solvent exchange rate but did not stop the diafiltration. Obviously, change of initial polymer concentration had a significant effect on the nanoscopic particle diameter. The solvent exchange using TFF ran smoothly over a wide range of hydrophobic/hydrophilic block ratios. However, at ratios higher than 6, the rapid addition of buffer resulted in precipitation of nanoparticles, which hindered further purification and required system

clean-up. Under these circumstances, one might consider using membranes with smaller pores or decreasing the process pressure to limit the buffer addition rate and alleviate the precipitation issue.

The experimental setup was designed with materials that had considerable chemical resistance to many aggressive organic solvents. In the future, the use of the system could be expanded beyond solvent exchange to conduct small-molecule removal, scale-up, and concentration processes on a wide range of polymers. For example, following the crosslinking of micelles during SCKs fabrication, the DFS can be used to remove urea byproducts and excess crosslinking agents. In addition, optimal operational parameters such as transmembrane pressure and circulation flow rate could be explored in more detail for any polymeric nanoparticles suspension using the system.

REFERENCES

1. Thurmond, K. B.; Kowalewski, T.; Wooley, K. L. *J. o. t. A. C. S.*, Water-soluble knedel-like structures: the preparation of shell-cross-linked small particles. **1996**, *118* (30), 7239-7240.
2. Thurmond, K. B.; Kowalewski, T.; Wooley, K. L. *J. o. t. A. C. S.*, Shell cross-linked knedels: A synthetic study of the factors affecting the dimensions and properties of amphiphilic core-shell nanospheres. **1997**, *119* (28), 6656-6665.
3. Lee, N. S.; Lin, L. Y.; Neumann, W. L.; Freskos, J. N.; Karwa, A.; Shieh, J. J.; Dorshow, R. B.; Wooley, K. L. *J. S.*, Influence of nanostructure morphology on host capacity and kinetics of guest release. **2011**, *7* (14), 1998-2003.
4. Wooley, K. L. *J. J. o. P. S. P. A. P. C.*, Shell crosslinked polymer assemblies: nanoscale constructs inspired from biological systems. **2000**, *38* (9), 1397-1407.
5. Huang, H.; Kowalewski, T.; Remsen, E. E.; Gertzmann, R.; Wooley, K. L. *J. J. o. t. A. C. S.*, Hydrogel-coated glassy nanospheres: a novel method for the synthesis of shell cross-linked knedels. **1997**, *119* (48), 11653-11659.
6. Patin, S. A., *Environmental impact of the offshore oil and gas industry*. JSTOR: 1999; Vol. 1.
7. Dave, D.; Ghaly, A. E., Remediation technologies for marine oil spills: A critical review and comparative analysis. *American Journal of Environmental Sciences* **2011**, *7* (5), 423.
8. Al-Majed, A. A.; Adebayo, A. R.; Hossain, M. E., A sustainable approach to controlling oil spills. *Journal of environmental management* **2012**, *113*, 213-227.
9. Pavia-Sanders, A.; Zhang, S.; Flores, J. A.; Sanders, J. E.; Raymond, J. E.; Wooley, K. L. *J. A. n.*, Robust magnetic/polymer hybrid nanoparticles designed for crude oil entrapment and recovery in aqueous environments. **2013**, *7* (9), 7552-7561.
10. Hickey, R. J.; Haynes, A. S.; Kikkawa, J. M.; Park, S.-J. *J. J. o. t. A. C. S.*, Controlling the self-assembly structure of magnetic nanoparticles and amphiphilic block-copolymers: from micelles to vesicles. **2011**, *133* (5), 1517-1525.
11. Davis, K. A.; Charleux, B.; Matyjaszewski, K. *J. J. o. P. S. P. A. P. C.*, Preparation of block copolymers of polystyrene and poly (t-butyl acrylate) of various molecular weights and architectures by atom transfer radical polymerization. **2000**, *38* (12), 2274-2283.
12. Sun, S.; Zeng, H.; Robinson, D. B.; Raoux, S.; Rice, P. M.; Wang, S. X.; Li, G. *J. J. o. t. A. C. S.*, Monodisperse mfe₂o₄ (m= fe, co, mn) nanoparticles. **2004**, *126* (1), 273-279.
13. Flores, J. A.; Pavia-Sanders, A.; Chen, Y.; Pochan, D. J.; Wooley, K. L., Recyclable hybrid inorganic/organic magnetically active networks for the sequestration of crude oil from aqueous environments. *Chemistry of Materials* **2015**, *27* (10), 3775-3782.
14. Kim, B.-S.; Qiu, J.-M.; Wang, J.-P.; Taton, T. A. *J. N. l.*, Magnetomicelles: composite nanostructures from magnetic nanoparticles and cross-linked amphiphilic block copolymers. **2005**, *5* (10), 1987-1991.

15. Liu, R.; Priestley, R. D. J. J. o. M. C. A., Rational design and fabrication of core-shell nanoparticles through a one-step/pot strategy. **2016**, *4* (18), 6680-6692.
16. Rolland, A., Clinical pharmacokinetics of doxorubicin in hepatoma patients after a single intravenous injection of free or nanoparticle-bound anthracycline. *International journal of pharmaceutics* **1989**, *54* (2), 113-121.
17. Fallouh, N. A. K.; Roblot-Treupel, L.; Fessi, H.; Devissaguet, J. P.; Puisieux, F., Development of a new process for the manufacture of polyisobutylcyanoacrylate nanocapsules. *International Journal of Pharmaceutics* **1986**, *28* (2-3), 125-132.
18. Krause, H.-J.; Schwarz, A.; Rohdewald, P., Interfacial polymerization, a useful method for the preparation of polymethylcyanoacrylate nanoparticles. *Drug development and industrial pharmacy* **1986**, *12* (4), 527-552.
19. Murakami, H.; Kobayashi, M.; Takeuchi, H.; Kawashima, Y., Preparation of poly(DL-lactide-co-glycolide) nanoparticles by modified spontaneous emulsification solvent diffusion method. *International Journal of Pharmaceutics* **1999**, *187* (2), 143-152.
20. Allemann, E.; Doelker, E.; Gurny, R., DRUG LOADED POLY(LACTIC ACID) NANOPARTICLES PRODUCED BY A REVERSIBLE SALTING-OUT PROCESS - PURIFICATION OF AN INJECTABLE DOSAGE FORM. *European Journal of Pharmaceutics and Biopharmaceutics* **1993**, *39* (1), 13-18.
21. Beck, P.; Scherer, D.; Kreuter, J., Separation of drug-loaded nanoparticles from free drug by gel filtration. *Journal of microencapsulation* **1990**, *7* (4), 491-496.
22. Szoka, F.; Papahadjopoulos, D., Procedure for preparation of liposomes with large internal aqueous space and high capture by reverse-phase evaporation. *Proceedings of the national academy of sciences* **1978**, *75* (9), 4194-4198.
23. Legrand, P.; Lesieur, S.; Bochot, A.; Gref, R.; Raatjes, W.; Barratt, G.; Vauthier, C., Influence of polymer behaviour in organic solution on the production of polylactide nanoparticles by nanoprecipitation. *International Journal of Pharmaceutics* **2007**, *344* (1-2), 33-43.
24. Govender, T.; Stolnik, S.; Garnett, M. C.; Illum, L.; Davis, S. S., PLGA nanoparticles prepared by nanoprecipitation: drug loading and release studies of a water soluble drug. *Journal of Controlled Release* **1999**, *57* (2), 171-185.
25. Miller, J. B.; Harris, J. M.; Hobbie, E. K., Purifying colloidal nanoparticles through ultracentrifugation with implications for interfaces and materials. *Langmuir* **2014**, *30* (27), 7936-7946.
26. Bertholon, I.; Vauthier, C.; Labarre, D., Complement activation by core-shell poly(isobutylcyanoacrylate)-polysaccharide nanoparticles: Influences of surface morphology, length, and type of polysaccharide. *Pharmaceutical Research* **2006**, *23* (6), 1313-1323.
27. Bouchemal, K.; Ponchell, G.; Mazzaferro, S.; Campos-Requena, V.; Gueutin, C.; Palmieri, G. F.; Vauthier, C., A new approach to determine loading efficiency of Leu-enkephalin in poly(isobutylcyanoacrylate) nanoparticles coated with thiolated chitosan. *Journal of Drug Delivery Science and Technology* **2008**, *18* (6), 392-397.
28. Vauthier, C.; Bouchemal, K., Methods for the Preparation and Manufacture of Polymeric Nanoparticles. *Pharmaceutical Research* **2009**, *26* (5), 1025-1058.

29. Limayem, I.; Charcosset, C.; Fessi, H., Purification of nanoparticle suspensions by a concentration/diafiltration process. *Separation and Purification Technology* **2004**, *38* (1), 1-9.
30. Tishchenko, G.; Luetzow, K.; Schauer, J.; Albrecht, W.; Bleha, M., Purification of polymer nanoparticles by diafiltration with polysulfone/hydrophilic polymer blend membranes. *Separation and Purification Technology* **2001**, *22-3* (1-3), 403-415.
31. Tishchenko, G.; Hilke, R.; Albrecht, W.; Schauer, J.; Luetzow, K.; Pientka, Z.; Bleha, M., Ultrafiltration and microfiltration membranes in latex purification by diafiltration with suction. *Separation and Purification Technology* **2003**, *30* (1), 57-68.
32. Theodore, L.; Ricci, F., *Mass transfer operations for the practicing engineer*. Wiley Online Library: 2010.
33. Robertson, J. D.; Rizzello, L.; Avila-Olias, M.; Gaitzsch, J.; Contini, C.; Magoń, M. S.; Renshaw, S. A.; Battaglia, G., Purification of nanoparticles by size and shape. *Scientific reports* **2016**, *6*, 27494.
34. Adjalle, K.; Tyagi, R.; Brar, S.; Valero, J.; Surampalli, R., Recovery of entomotoxicity components from *Bacillus thuringiensis* fermented wastewater and sludge: Ultrafiltration scale-up approach. *Separation and Purification Technology* **2009**, *69* (3), 275-279.
35. Harmant, P.; Aimar, P., Coagulation of colloids retained by porous wall. *AIChE journal* **1996**, *42* (12), 3523-3532.
36. Madaeni, S.; Fane, A., Microfiltration of very dilute colloidal mixtures. *Journal of Membrane Science* **1996**, *113* (2), 301-312.
37. Casey, C.; Gallos, T.; Alekseev, Y.; Ayturk, E.; Pearl, S., Protein concentration with single-pass tangential flow filtration (SPTFF). *Journal of membrane science* **2011**, *384* (1-2), 82-88.
38. Kendall, D.; Lye, G.; Levy, M., Purification of plasmid DNA by an integrated operation comprising tangential flow filtration and nitrocellulose adsorption. *Biotechnology and bioengineering* **2002**, *79* (7), 816-822.
39. Negrete, A.; Pai, A.; Shiloach, J., Use of hollow fiber tangential flow filtration for the recovery and concentration of HIV virus-like particles produced in insect cells. *Journal of virological methods* **2014**, *195*, 240-246.
40. Pansare, V. J.; Tien, D.; Thoniyot, P.; Prud'homme, R. K., Ultrafiltration of nanoparticle colloids. *Journal of Membrane Science* **2017**, *538*, 41-49.
41. He, Z.; Hu, Y.; Nie, T.; Tang, H.; Zhu, J.; Chen, K.; Liu, L.; Leong, K. W.; Chen, Y.; Mao, H.-Q., Size-controlled lipid nanoparticle production using turbulent mixing to enhance oral DNA delivery. *Acta biomaterialia* **2018**, *81*, 195-207.
42. Dalwadi, G.; Benson, H. A.; Chen, Y., Comparison of diafiltration and tangential flow filtration for purification of nanoparticle suspensions. *Pharmaceutical research* **2005**, *22* (12), 2152-2162.
43. Dalwadi, G.; Sunderland, V. B., Purification of PEGylated nanoparticles using tangential flow filtration (TFF). *Drug development and industrial pharmacy* **2007**, *33* (9), 1030-1039.

44. Hirsjärvi, S.; Peltonen, L.; Hirvonen, J., Effect of sugars, surfactant, and tangential flow filtration on the freeze-drying of poly (lactic acid) nanoparticles. *Aaps Pharmscitech* **2009**, *10* (2), 488-494.
45. Van Reis, R.; Gadam, S.; Frautschy, L. N.; Orlando, S.; Goodrich, E. M.; Saksena, S.; Kuriyel, R.; Simpson, C. M.; Pearl, S.; Zydney, A. L., High performance tangential flow filtration. *Biotechnology and bioengineering* **1997**, *56* (1), 71-82.
46. Zaloga, J.; Stapf, M.; Nowak, J.; Pöttler, M.; Friedrich, R.; Tietze, R.; Lyer, S.; Lee, G.; Odenbach, S.; Hilger, I., Tangential flow ultrafiltration allows purification and concentration of lauric acid-/albumin-coated particles for improved magnetic treatment. *International journal of molecular sciences* **2015**, *16* (8), 19291-19307.
47. Quintanar-Guerrero, D.; Ganem-Quintanar, A.; Allémann, E.; Fessi, H.; Doelker, E., Influence of the stabilizer coating layer on the purification and freeze-drying of poly (D, L-lactic acid) nanoparticles prepared by an emulsion-diffusion technique. *Journal of Microencapsulation* **1998**, *15* (1), 107-119.
48. Sun, B.; Yu, X. H.; Yin, Y. H.; Liu, X. T.; Wu, Y. G.; Chen, Y.; Zhang, X. Z.; Jiang, C. L.; Kong, W., Large-scale purification of pharmaceutical-grade plasmid DNA using tangential flow filtration and multi-step chromatography. *J. Biosci. Bioeng.* **2013**, *116* (3), 281-286.
49. van Reis, R.; Leonard, L. C.; Hsu, C. C.; Builder, S. E., Industrial scale harvest of proteins from mammalian cell culture by tangential flow filtration. *Biotechnology and bioengineering* **1991**, *38* (4), 413-422.
50. Borger, V.; Dittrich, R.; Staubach, S.; Zumegen, S.; Horn, P.; Giebel, B., TANGENTIAL FLOW FILTRATION, A POTENTIAL METHOD FOR THE SCALED PREPARATION OF EXTRACELLULAR VESICLES. *Cytotherapy* **2019**, *21* (5), S57-S57.
51. Tutunjian, R. S., Scale-up considerations for membrane processes. *Bio/Technology* **1985**, *3* (7), 615.
52. Aminabhavi, T. M.; Gopalakrishna, B., Density, viscosity, refractive index, and speed of sound in aqueous mixtures of N, N-dimethylformamide, dimethyl sulfoxide, N, N-dimethylacetamide, acetonitrile, ethylene glycol, diethylene glycol, 1, 4-dioxane, tetrahydrofuran, 2-methoxyethanol, and 2-ethoxyethanol at 298.15 K. *Journal of Chemical and Engineering Data* **1995**, *40* (4), 856-861.
53. Jouyban, A.; Soltanpour, S.; Chan, H.-K., A simple relationship between dielectric constant of mixed solvents with solvent composition and temperature. *International journal of pharmaceutics* **2004**, *269* (2), 353-360.
54. Rosenberg, E.; Hepbildikler, S.; Kuhne, W.; Winter, G. J. J. o. M. S., Ultrafiltration concentration of monoclonal antibody solutions: Development of an optimized method minimizing aggregation. **2009**, *342* (1-2), 50-59.
55. Zhang, L.; Eisenberg, A., Thermodynamic vs kinetic aspects in the formation and morphological transitions of crew-cut aggregates produced by self-assembly of polystyrene-b-poly (acrylic acid) block copolymers in dilute solution. *Macromolecules* **1999**, *32* (7), 2239-2249.
56. Mai, Y.; Eisenberg, A., Self-assembly of block copolymers. *Chemical Society Reviews* **2012**, *41* (18), 5969-5985.

APPENDIX A

HYDRODYNAMIC SIZE MEASUREMENTS (DLS)

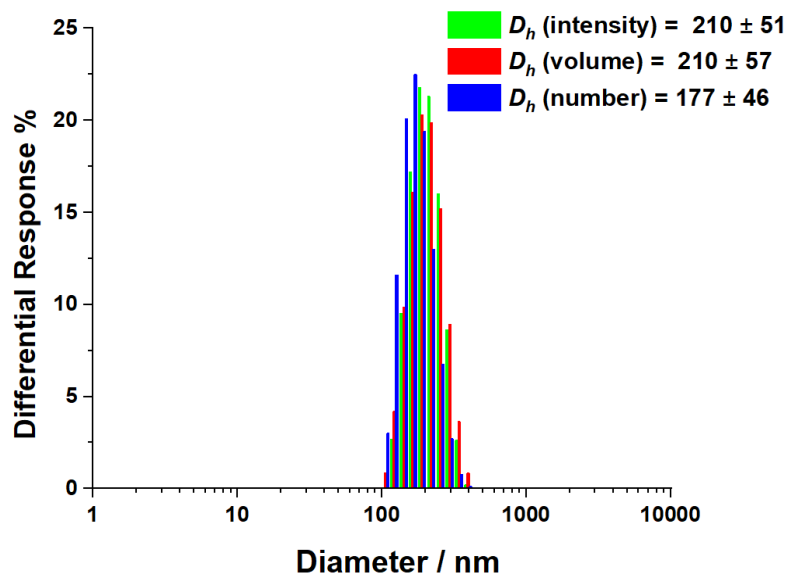


Figure A.1. PAA₄₇-*b*-PS₂₃₅ (1.0 mg/mL, P_R=10 psig)

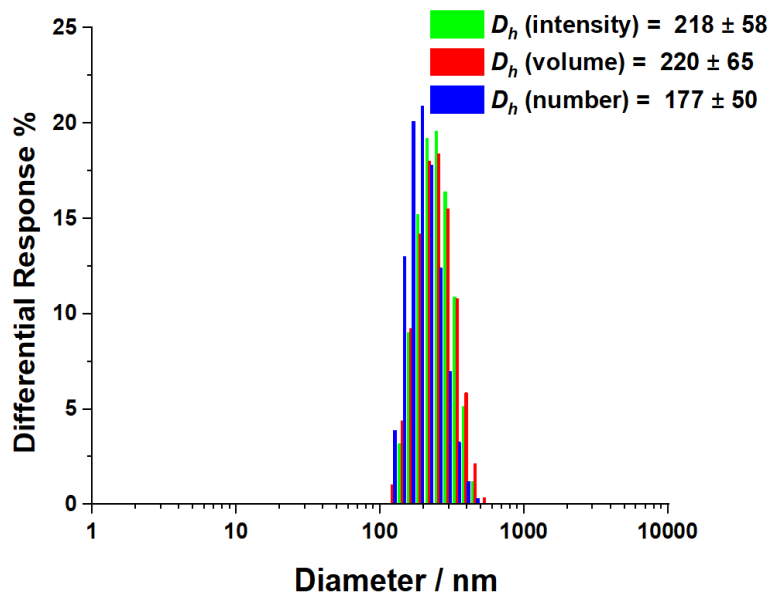


Figure A.2. PAA₄₇-*b*-PS₂₃₅ (1.0 mg/mL, P_R=20 psig)

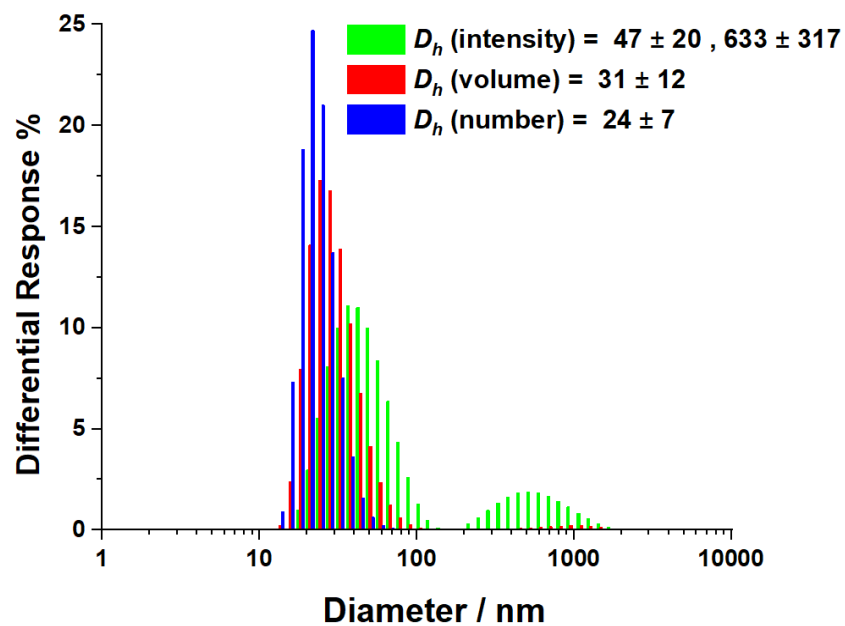


Figure A.3. PAA₆₄-*b*-PS₆₀ (1.0 mg/mL, P_R=20 psig)

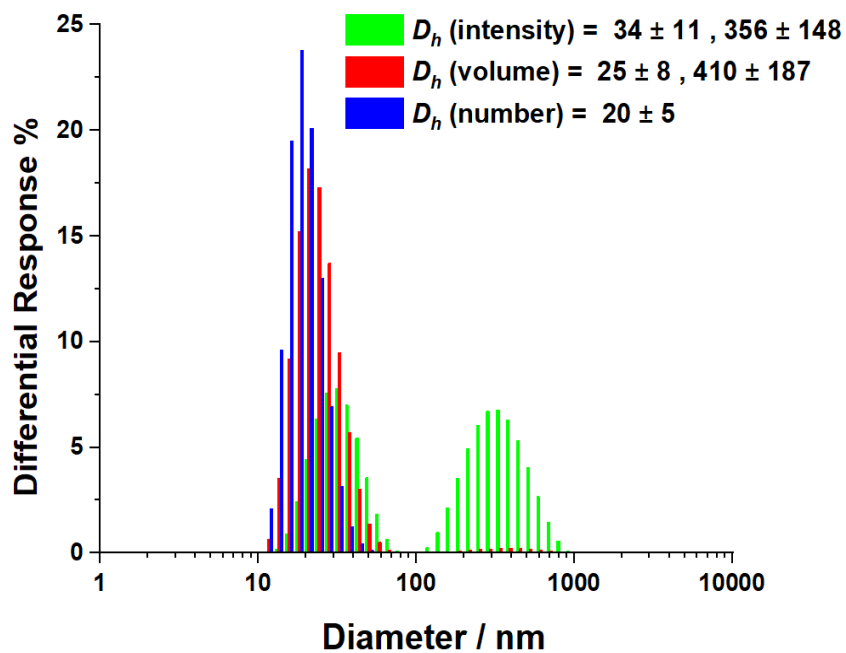


Figure A.4. PAA₂₂-*b*-PS₁₄₁ (2.5 mg/mL, P_R=20 psig)

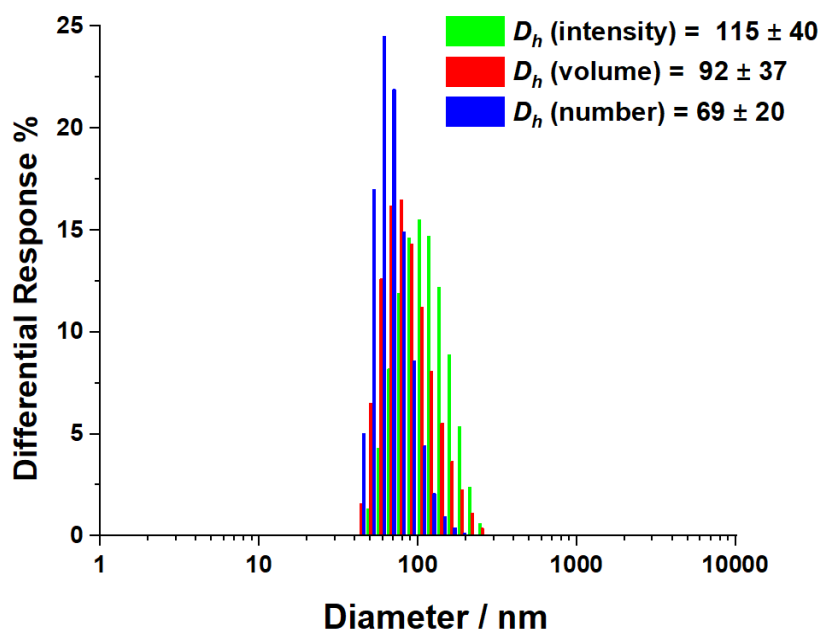


Figure A.5. PAA₈₅-*b*-PS₁₈₂ (1.0 mg/mL, P_R=20 psig)

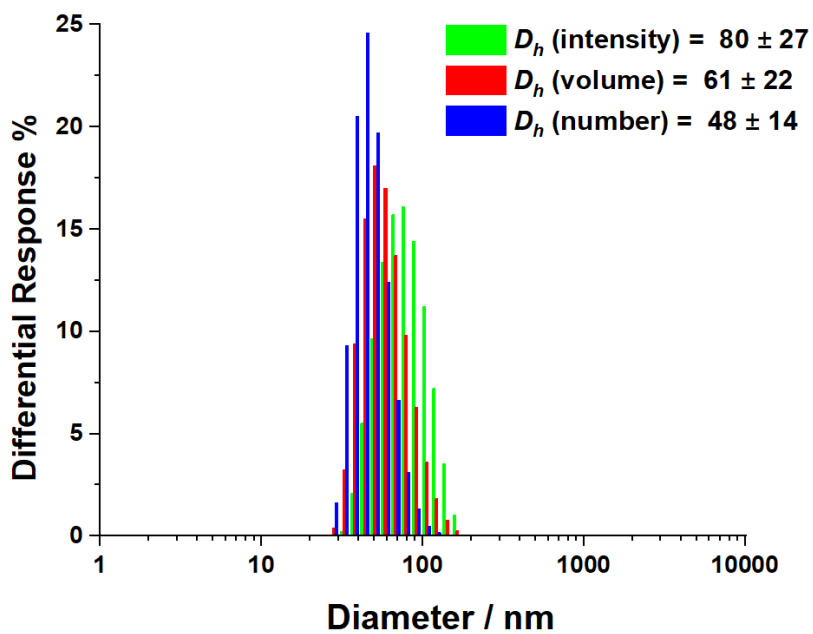


Figure A.6. PAA₈₅-*b*-PS₁₈₂ (1.0 mg/mL)-Batch

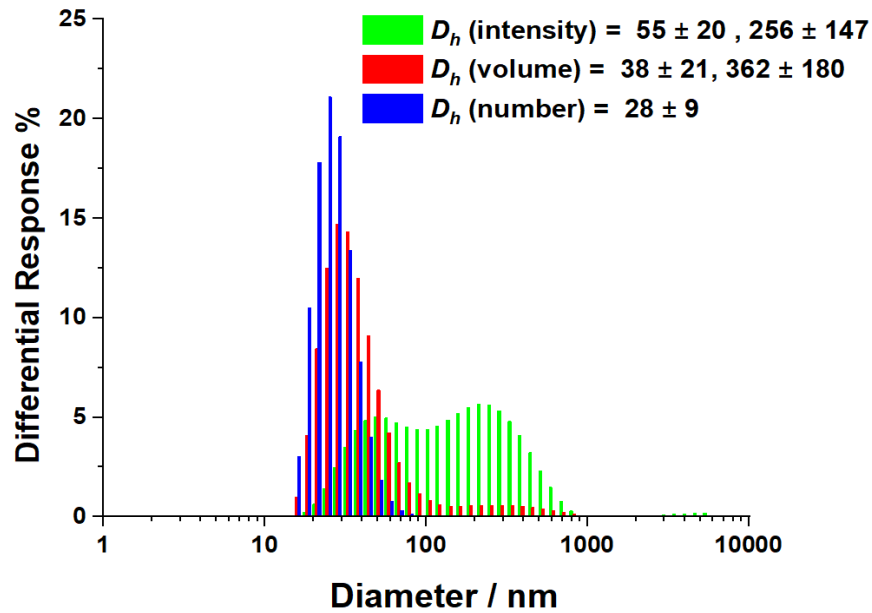


Figure A.7. PAA₆₄-*b*-PS₆₀ (2.5 mg/mL, P_R=20 psig)

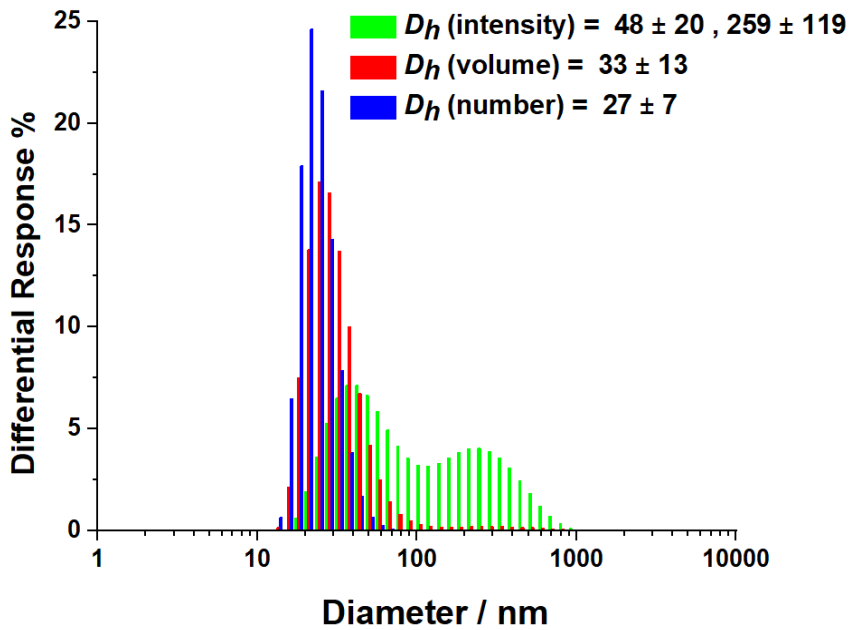


Figure A.8. PAA₆₄-*b*-PS₆₀ (2.5 mg/mL)-Batch

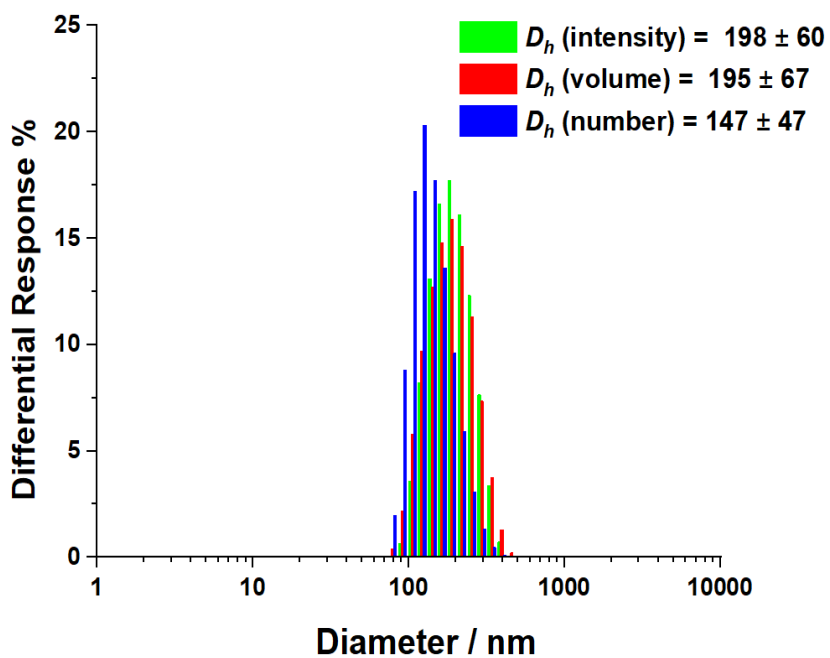


Figure A.9. PAA₄₇-b-PS₂₃₅ (2.5 mg/mL, P_R=20 psig)

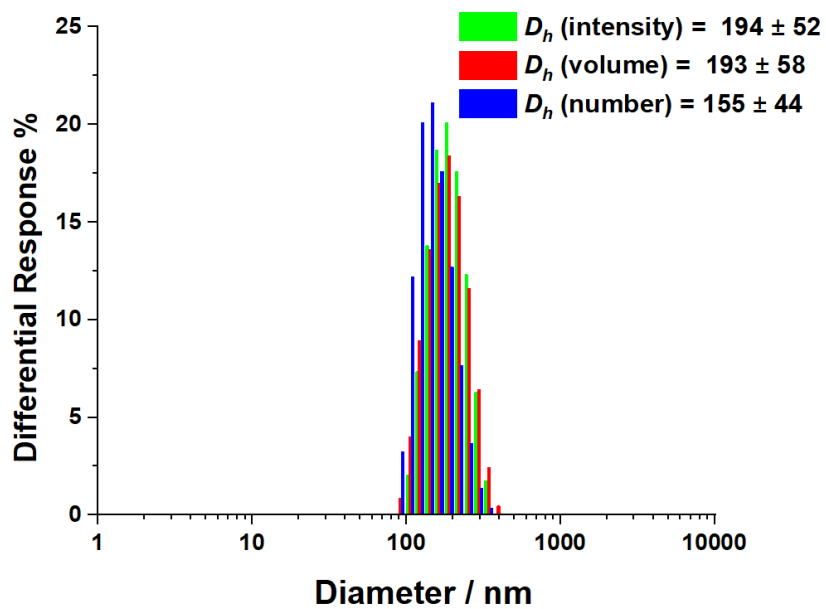


Figure A.10. PAA₄₇-b-PS₂₃₅ (2.5 mg/mL)-Batch

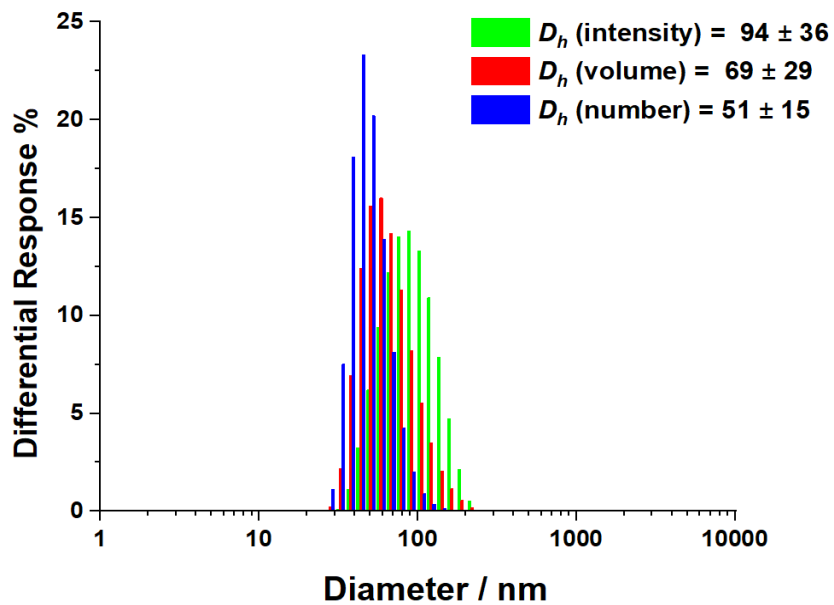


Figure A.11. PAA₆₄-*b*-PS₆₀ (4.0 mg/mL, P_R=20 psig)

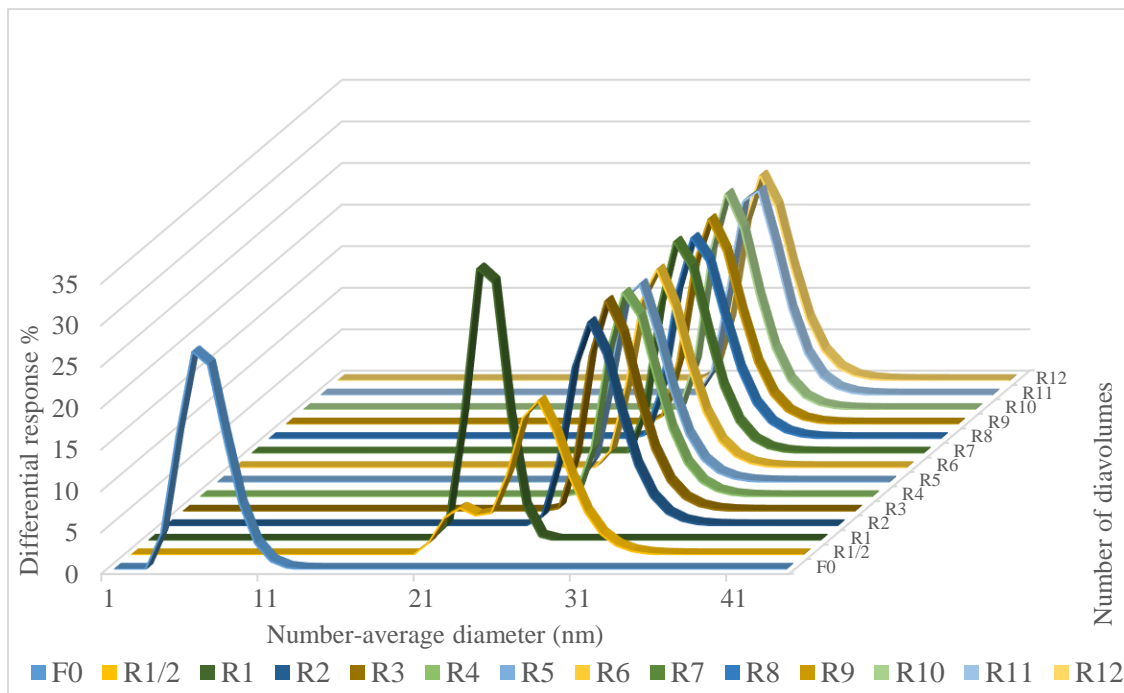


Figure A.12. Particle diameter distribution evolution over time during diafiltration of

PAA₆₄-*b*-PS₆₀ (1.0 mg/mL)

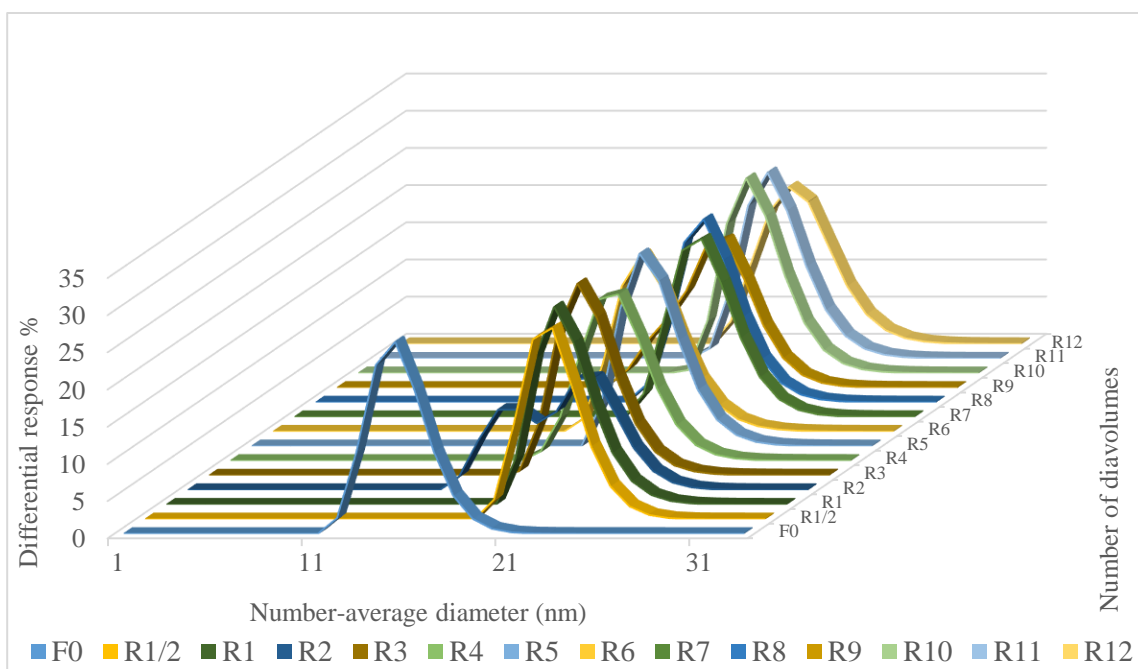


Figure A.13. Particle diameter distribution evolution over time during diafiltration of PAA₆₄-b-PS₆₀ (2.5 mg/mL)

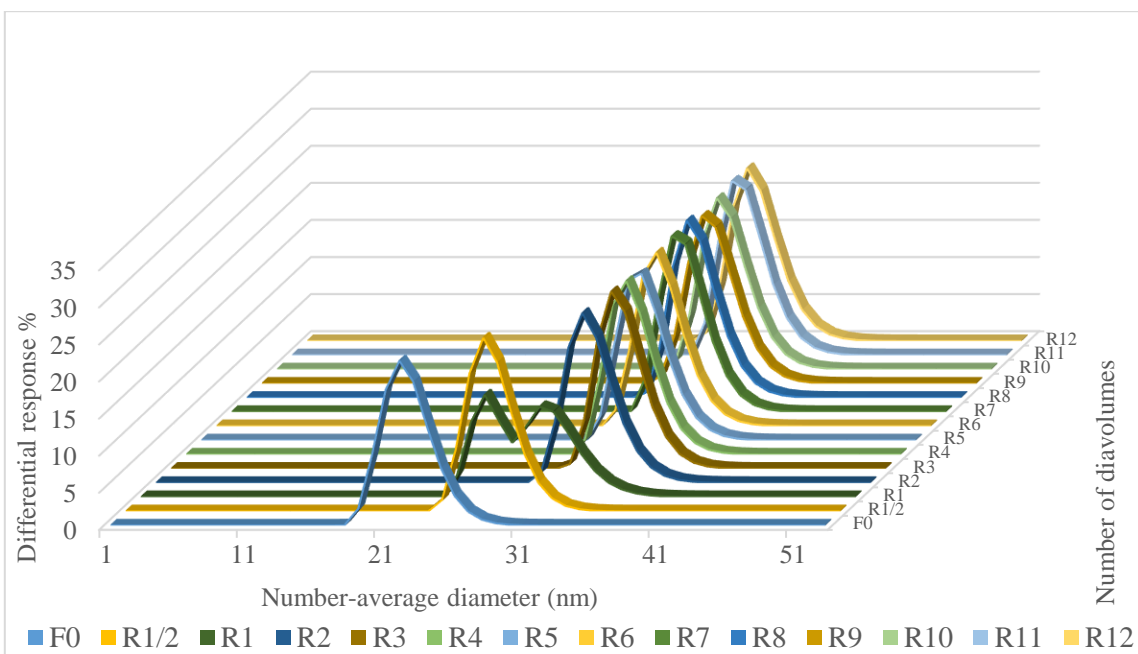


Figure A.14. Particle diameter distribution evolution over time during diafiltration of PAA₆₄-b-PS₆₀ (4.0 mg/mL)

APPENDIX B
NOMENCLATURE

AFM	Atomic force microscopy
ATRP	Atom transfer radical polymerization
CuBr	Copper(I) bromide
DCM	Dichloromethane
DFS	Diafiltration system
DLS	Dynamic light scattering
GC-MS	Gas chromatography-mass spectrometry
GPC	Gel permeation chromatography
FPT	Freeze-pump-thaw
FTIR	Fourier transform infrared
HSGC	Headspace gas chromatography
MWCO	Molecular weight cutoff
PAA	Poly(acrylic acid)
P_F	Feed pressure
P_R	Retentate pressure
PMDETA	<i>N,N,N',N',N''</i> -pentamethyldiethylenetriamine
PS	Polystyrene
Psi	Pounds per square inch
Psig	Pounds per square inch gauge

PtBA	Poly(<i>tert</i> -butyl acylate)
SCK	Shell crosslinked knedel-like
SEC	Size exclusion chromatography
TEM	Transmission electron microscopy
TFA	Trifluoroacetic acid
TFF	Tangential flow filtration
THF	Tetrahydrofuran
TMP	Transmembrane pressure